

THE MECHANISM OF ACCELERATED HYDROLYTIC AGING ON SILICONE
ADHESIVE

By

Wanru Miao

A THESIS

Submitted to
Michigan State University
in partial fulfillment of the requirements
for the degree of

Civil Engineering—Master of Science

2020

ABSTRACT

THE MECHANISM OF ACCELERATED HYDROLYTIC AGING ON SILICONE ADHESIVE

By

Wanru Miao

Silicone adhesive is conspicuous by its bonding properties, rubbery behavior, and high surface tensile strength, but it is capable of being damaged by exposure to harsh environments. Moisture and temperature were considered as imperative environmental factors in natural aging. Thus, accelerated hydrolytic aging was conducted in the laboratory to investigate the mechanism of degradation of Polydimethylsiloxane (PDMS)-based adhesive. Desalinated water and salinated water as prevailing aqueous environments were chosen for the experiments. Deterioration was evaluated by weight changes, mechanical behaviors, visual inspections, FT-IR (Fourier-Transform Infrared) Spectroscopy, DMA (Dynamic Mechanical Analysis), and SEM (Scanning Electron Microscopy) tests. Increasing water uptake is proportional to decreasing tensile strength and escalation of elongation at break after desalinated water immersion. This phenomenon is indicated as a continued expansion of plasticization, which mainly reflects the reduction of T_g . In the case of salinated water, water uptakes of specimens were impeded by sea salt. This research is designated to cope with the application of silicone sealant in harsh environments.

TABLE OF CONTENTS

LIST OF TABLES	i
LIST OF FIGURES	ii
1 CHAPTER 1: Introduction	1
1.1 Aging.....	2
1.2 Hydrolytic aging	3
1.3 PDMS.....	5
1.4 Constitutive behavior	7
1.5 Mullins effect	8
1.6 Physic-chemical changes	9
1.7 Literature review	10
2 CHAPTER 2: Materials and Methods	12
2.1 Experimental design.....	12
2.2 Sample preparation	12
2.3 Accelerated hydrolytic aging	13
2.4 Water uptake	14
2.5 Mechanical tests.....	14
2.6 FT-IR.....	16
2.7 DMA	17
2.8 SEM	18
3 Chapter 3: Test Results and Discussion.....	19
3.1 Water uptake	19
3.2 Mechanical properties	20
3.2.1 Tensile failure tests	20
3.2.2 Tensile cyclic tests	27
3.3 FT-IR analysis.....	32
3.3 DMA analysis	36
3.4 SEM analysis	41
4 Conclusion	43
5 Future Work	45
Bibliography	47

LIST OF TABLES

Table 1 Assignments and wave ranges corresponding to FT-IR spectra pinnacles.....	35
Table 2 The water uptake and T_g of specimens for desalinated water under various temperatures.	39

LIST OF FIGURES

Figure 1.1 The hydrolyzed PDMS to form VMS.	4
Figure 1.2 The chemical composition of PDMS.	6
Figure 1.3 The hydrolysis reaction of PDMS.	7
Figure 1.4 The backbiting reactions and depolymerization of PDMS.....	7
Figure 2.1 Mold for sample preparation	13
Figure 2.2 Standard dimension for dog-bone samples.....	13
Figure 2.3 A schematic container to display immersion situation.....	14
Figure 2.4 Tensile machine with roller grips.	15
Figure 2.5 A schematic curve for cyclic test.....	16
Figure 2.6 Jasco FT/IR - 4600 spectrometer.....	16
Figure 2.7 TA Instrument DMA Q800 machine.....	17
Figure 3.1 Water uptake under temperature superposition for (a) desalinated water and (b) salinated water.	19
Figure 3.2 Temperature comparison for (a) tensile strength and (b) elongation at break of samples submerged within desalinated water.	20
Figure 3.3 Duration comparison for (a) tensile strength and (b) elongation at break with immersion of desalinated water.	21
Figure 3.4 Temperature comparison for (a) tensile strength and (b) elongation at break within salinated water.	22
Figure 3.5 Duration comparison for (a) tensile strength and (b) elongation at break within salinated water.	23
Figure 3.6 Comparison between influence of desalinated and salinated water on specimens of (a) tensile strength and (b) elongation at break at 60°C.....	23
Figure 3.7 Comparison between influence of desalinated and salinated water on specimens of (a) tensile strength and (b) elongation at break at 80°C.....	24
Figure 3.8 Comparison between influence of desalinated and salinated water on specimens of (a) tensile strength and (b) elongation at break at 95°C.....	25

Figure 3.9 The stress-strain curves of specimens for (a) desalinated water and (b) salinated water.	26
Figure 3.10 (a) Schematic representations for relative stress softening, relative residual strain and hysteresis loss and (b) Stress- strain curve of cyclic tensile test of virgin specimens.	28
Figure 3.11 Relative stress softening for (a) desalinated water, and (b) salinated water in 87% strain.....	29
Figure 3.12 Relative residual strain for (a) desalinated water, and (b) salinated water in 87% strain.....	30
Figure 3.13 Hysteresis loss for (a) desalinated water, and (b) salinated water in 87% strain.	31
Figure 3.14 The FT-IR spectra of virgin and aged specimens through various durations and temperatures within (a) desalinated water and (b) salinated water.	36
Figure 3.15 Storage modulus variation aged within (a)desalinated water and (b) salinated water, loss modulus changes of (c) desalinated water and (d) salinated water and Tan δ changed due to (e)desalinated water and (f) salinated water aging.	40
Figure 3.16 Glass transition temperature changed after (a) desalinated water, and (b) salinated water aging.....	41
Figure 3.17 Failure samples and SEM micro-graphs of tensile fracture surfaces of (a), (b), and (c) virgin specimens, (d), (e), and (f) specimens aged within desalinated water at 95°C for 30 days, and (g), (h), and (i) specimens aged within salinated water at 95°C for 30 days.	43

1 CHAPTER 1: Introduction

Adhesives, specifically elastomeric adhesives, are becoming widespread in many applications due to their unique and interesting characteristics, such as flexibility, elasticity, resistance to heat, moisture, and chemical substances. Adhesives have considerable advantage over more conventional methods of assembly like bolts and rivets, since they facilitate stress distribution at the joints, reduce the cost of sealing, and promote the aesthetic design of structures. Thus, adhesives are capable of widely applying in aerospace, electronic field, medical treatment, and construction industries (Keshavaraj, 1994) (Yanagibashi, 1990). Adhesives play an imperative role in bonding two various materials with different properties, like plastic and glass or even composites and metals. Due to their great thermal and moisture resistance, adhesives usually are used in harsh environment applications. Being exposed to harsh environment for a long time cause the mechanical behavior of adhesives to change, a process generally known as aging. Therefore, in order to make sure of the safety of the structure, inspecting the adhesive bonds is a must. Of course, there are some applications such as offshore and underwater applications that the adhesives may often be out of reach, where visual inspection is not always an option. Hence accurate understanding of adhesive service life reduction due to aging, especially in the hydrolytic aging, is of utmost significance to prevent disastrous events heading in harm's way. Consequently, many researchers investigated the degradation process and apply it in various fields. Although the weather degradation of polymers has been studied for decades, there is still no concrete model that can perfectly predict the effects of aging on adhesives behavior. Therefore, it necessitates further investigation in this direction to better understand the impact of this phenomenon on adhesives' behaviors.

1.1 Aging

Aging is defined as a degradation mechanism caused by weathering factors, which displays in alteration of mechanical behaviors, the texture of surfaces, and composition of materials. When exposing to actual environments for long periods, adhesives might undergo degradation owing to ultraviolet light, high temperature, moisture, oxygen, or their combinations (Mohammadi, 2019). More specifically, aging can be categorized into thermal-oxidation, photo-oxidation, hygro-thermal. Those aging combinations are capable of implementing more severe deterioration of materials, termed as accelerated aging, than single aging process. The aging mechanisms are capable of inciting physical and chemical deterioration over time (Barbosa, 2017). Physical alterations embody the changes in the molecular conformation rather than the structural integrity of the materials, which is regarded as reversible changes (Tavares, 2003). While chemical changes, an irreversible mechanism, issue from altering material chain structure at the molecular level upon long-term exposure (Celina, 2013).

As aforementioned, physical aging plays an imperative role in the material aging process (Tavares, 2003) (Bahrololoumi, 2020). The physical aging is manifested when polymers are cooled from the temperatures above to below T_g , which would lead to the non-equilibrium states inside of materials (Hutchinson, Physical aging of polymers, 1995). Afterward, the evolution towards thermodynamic equilibrium is occurred to generate driving forces for the changes of volume, toughness, viscoelasticity, and permeability (Odegard, 2011) (Hutchinson, 1995). As a reversible process, the aged materials could be heated above T_g and then restore the degraded properties to its original state (McCaig, 1999). Given chemical aging, oxidation (Gulmine, 2003) (Khabbaz, 1999) and hydrolysis (Montes, 2012) (Sedenkova, 2008) are regarded as aging procedures that would cause the changes on the macrostructures, including the occurrences of

chain scission and cross-links, subsequently or simultaneously. Oxidation is interpreted as the disintegration of macromolecules by the presence and action of oxygen on the materials to form free radicals (Izdebska, 2015). Hydrolysis is defined as a chemical reaction that water breaks the bond of materials and change the macromolecular structures, which mostly occurs in the hydrolytic aging. In most weathering circumstances, physical and chemical aging simultaneously engender the structural variation of materials.

1.2 Hydrolytic aging

To gain an exhaustive knowledge of deterioration of rubberlike materials due to aging, aging process has been divided into various directions. The hydrolytic aging can be interpreted as a kind of the aging procedures where materials are exposed to various liquid solutions for the long term, which induces a series of changes without involving oxidative influences. These governing phenomena in hydrolytic aging have been an impediment to the comprehension and understanding of singularities that cause swelling (Li X. a., 2004), cracking (Alessi, 2014), post-curing (Ma, 2018) and plasticization (Sang, 2018) taking place simultaneously or subsequently.

The swelling is a phenomenon compelled by which penetration of solvent into the materials network causes abrupt volume change (Gugliuzza, 2007). What's more, the level of swelling depends on the temperatures and immersion mediums. It is acknowledged that swelling of polymer increases as temperatures rise. Distilled water is more conducive to the proceeding of swelling than salt solution owing to hydrated ions and ionic atmospheres (Choi, 2010). Another phenomenon needed to be illustrated is plasticization, which makes materials more flexible and elastic. In prolonged hydrolytic aging, water or other mediums acting as a plasticizer penetrates into materials and cause plasticization, which is characterized by declining T_g (Capiel, 2017).

Plasticization is identified as physical transformations acting on the amorphous part of materials

to increase the mobility of chains so that elongation at break raises while the tensile strength declines (Levine, 1988). Specifically, plasticizer increases the free volume of polymer chains and reduces the frictions between chains during motions to cause mechanical changes. Moreover, while it affects the length distribution of polymer chains, further degradation emerges as a consequence of breakage of chemical bonds, which is regarded as a chemical alteration at the macromolecular level. The breakage of chemical bonds could cause the detachment of molecules from long chains. Those molecules could be trickled and migrated from materials by water or other solution mediums via a process termed as leaching (Rahman, 2004). On the other hand, in immersion environment with an appropriate catalyst, materials are able to generate new chemical bonds and form new crosslinks. For example, PDMS (polydimethylsiloxane), a kind of thermoset polymers, has been hydrolyzed to generate VMS (volatile methyl siloxane), a low-molecule-weight compound, which is displayed in Figure 1.1 (Accettola, 2008).

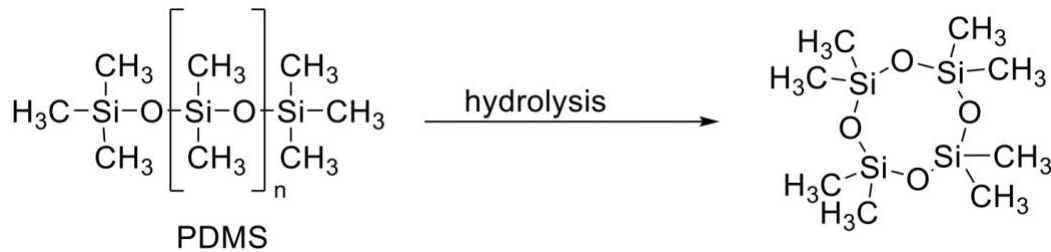


Figure 1.1 The hydrolyzed PDMS to form VMS.

Accelerated hydrolytic aging refers to a combination of hydrolytic aging and thermal aging to achieve long-term natural environmental effects on the material under consideration. Polymers after hydrolytic aging at elevated temperatures degrade not only by moisture but also by intense heat. Thermal aging plays a considerable role in the mechanism of accelerated hydrolytic aging. Cracking might occur since moisture diffuse into polymers through microcracks and voids, the defects of materials. Moisture would be transported by microcracks

and void, which triggers swelling of materials and stresses to form stress cracking (Awaja, Cracks, microcracks and fracture in polymer structures: Formation, detection, autonomic repair, 2016). Short-term aging at elevated temperatures and a certain level of moisture engenders which is attributed to post-curing with cross-linking (Wang, 2016) (Mathew, 2001). The entanglement of polymer chains and the chemical bonds between chains could be altered by the aging procedure. The intense heat can improve the motion of polymer chains and thus generate physical entanglement of chains. The polymer chains would be rearranged in the effect of heat. Under the aging of heat and moisture, polymer chains could occur physical changes, like cracking and swelling, and chemical changes, including breakage of chemical bonds and generate new crosslinks.

1.3 PDMS

Changes of materials after aging, especially accelerated hydrolytic aging, has been established. Nevertheless, influences of hydrolytic aging vary based on the different characteristics, physical properties and chemical compositions of materials. Changes of accelerated hydrolytic aging are needed to be explored in a specific material — PDMS (polydimethylsiloxane).

It is acknowledged that prevailing silicone-based adhesive is outlined as high permeability, low glass transition temperature, and high surface tension material (De Buyl, 2001). PDMS, shown in Figure 1.2, is a prevalent component of silicone adhesives. PDMS, a semi-crystalline polymer (Sundararajan, 2002), has been widely applied in the marine environment due to its hydrophobic property (Chen, 2019). PDMS displays high flexibility, elasticity, and heat resistance attributed to its Si-O bond (Le Gac, 2012). Therefore, PDMS

composites the silicone adhesives to be applied in various field, such as building construction bonding.

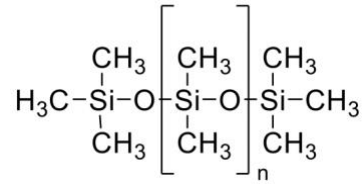


Figure 1.2 The chemical composition of PDMS.

In order to get rid of abrupt rupture of materials exposed to moisture and heat, it is necessary to study the accelerated hydrolytic aging exerted on PDMS. Swelling of PDMS occurs during the submersion of a solvent (Dangla, 2010). Aging at elevated temperatures might produce the increment of cross-link density inside PDMS, as aforementioned post-curing (Chaudhry, 2001). In the case of accelerated hydrolytic aging, the PDMS network would be rearranged and optimized to reach equilibrium in physical alteration in accordance with physical aging (Lewicki, The thermal degradation behavior of polydimethylsiloxane/montmorillonite nanocomposites, 2009) (Bele, 2016). On the other hand, for chemical changes, it is worth mentioning that the hydrolysis of PDMS could create an oligomeric product in an alkaline solution to form the denser colloidal aerogel shown in Figure 1.3 (Warrick, 1979) (Jagger, 2003). Aging at elevated temperatures, PDMS deteriorated by inter-molecular de-polymerization reactions, named back-biting, shown in Figure 1.4 (Lewicki, The thermal degradation behavior of polydimethylsiloxane/montmorillonite nanocomposites, 2009) (Grassie, 1978). Those chemical changes decrease the molecular weight to promote the constitution of volatile materials, which could have been broken by chain scission reactions(Xiang, 2012).

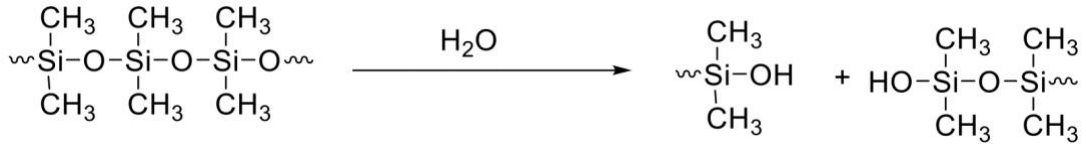


Figure 1.3 The hydrolysis reaction of PDMS.

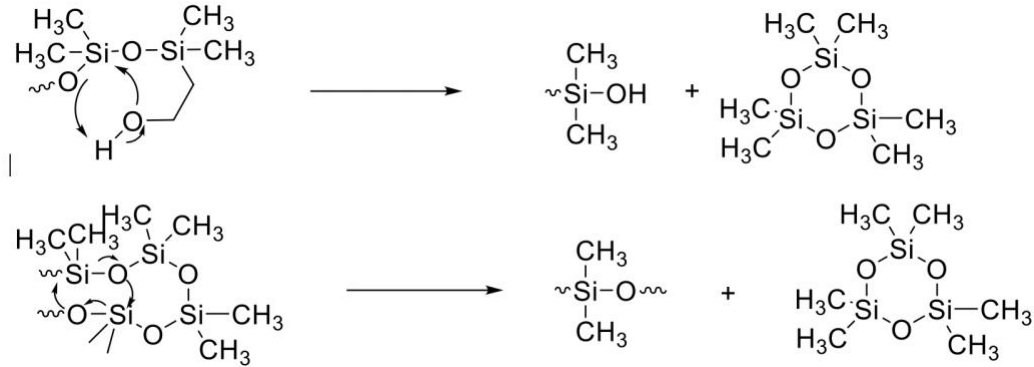


Figure 1.4 The backbiting reactions and depolymerization of PDMS.

1.4 Constitutive behavior

The physical and chemical changes induced by aging will directly influence the mechanical performances of materials. The level of degradation due to aging could be evaluated by the variation of mechanical behaviors of materials.

Constitutive behavior is the stress-strain behavior of rubberlike materials. The stress-strain curves of failure tests and cyclic tests can be termed as constitutive behaviors. Tensile failure tests exhibit the needed stress until sample breaks and its corresponding strain value. The constitutive behavior of materials is an effective manner to evaluate the degree of degradations in the respect of physic-chemical changes after desired-time aging. Aged specimens require high stress till break and could be extended to the similar level of virgin specimens, called hardening behavior, which represents the increment of the cross-link. If samples are aged under elevated temperatures for a short period, that phenomenon can be regarded as post-curing. On the contrary, the maximum stress of aged samples is less than unaged specimens, named softening

behaviors, which might be on account of the loss of crosslink. Once the reduction of tensile strength accompanies with increasing failure strain, plasticization might occur after immersed in solvents. Likewise, materials lose their ductility and tensile strength, titled brittle behavior, which generated by chain scissions and other changes induced by aging (Fayolle, 2008). The relative rate of polymer chain scission, sorption, and resulting cross-link density determines the subsequent hardening or softening behaviors of material. While these rates may be variable depending on material chemistry, aging condition, etc., it is expected that the resulting changes in cross-link density will demonstrate an exponentially changes, due to various aging, occurred within materials.

On the other hand, the stress-strain curves of cyclic tests can also be named as constitutive behaviors where the aged specimens would be deformed by tension or compression. Thus, materials are damaged by aging and cyclic deformations. The constitutive behavior of cyclic tests of specimens would exhibit the inelastic behaviors of materials. Various degradation induced by aging alter the inelastic behaviors, such as stress softening, which has been intensively studied by Mullins.

1.5 Mullins effect

Mullins compared mechanical behavior of unfilled and filled rubber and found the stress softening behaviors in filled rubber, which consequently is named as Mullins effect. Mullins effect is able to denote the inelastic behavior of rubber-like materials based on the performance of the first extension. Mullins effect has been mainly studied in filled rubber and thermoplastic rubber – polyurethane (Diani, A review on the Mullins effect, 2009). Stress softening, residual strain, and hysteresis can be regarded as three ways to evaluate inelastic behaviors. Firstly, stress softening is characterized as a reduction of stress after the first loading, when specimens reach

the same strain of the first load. This phenomenon was explained by Dannenberg, proposing the slippage of polymer chains on the fillers (E.M.Dannenberg, 1966). Secondly, what was mentioned by Mullins was the permanent set referred to as residual strain, which was residual extension of specimens after loading and unloading. Dorfmann and Ogden reported that residual strain would increase with the number of fillers and the stretching value applied to materials (Dorfmann, A constitutive model for the Mullins effect with permanent set in particle-reinforced rubber, 2004). Last but not least, hysteresis is the area of loading-unloading stress-strain curves. The hysteresis could be influenced by filled rubber viscoelasticity and crystallization, changes of macro-structures, loss of fillers aggregates (Harwood, 1971).

The structural changes of materials are relevant to the inelastic behaviors investigated by Mullins. And the structural changes will depend on aging process and material properties. Therefore, it is necessary to study the accelerated hydrolytic aging of PDMS-based adhesives on Mullins effect.

1.6 Physic-chemical changes

In order to further understand the damage induced by aging, physical and chemical changes are able to be detected by FT-IR (Fourier-Transform Infrared) Spectroscopy and DMA (Dynamic Mechanical Analysis) tests. The difference of morphology between virgin and aged specimens could be observed by SEM (Scanning Electron Microscopy) micrographs.

FT-IR is a potent technique to detect the functional groups on the polymer chains. The functional groups can be determined by the amount of light absorbed by samples. FT-IR machine measures the intensity of a certain range of wavelengths to form the spectra of the materials. Hence, the FT-IR could be utilized to capture the chemical changes of materials due to aging. DMA tests are used to obtain the physical change — plasticization. DMA machines calculate the

storage modulus, loss modulus and $\tan \delta$, which is based on the dynamic deformation of a desired stress or strain. There are three ways to determine T_g : the onset of storage modulus, and the peak point of loss modulus and $\tan \delta$. When T_g of aged specimens is less than virgin specimens, plasticization occurs during aging. SEM can capture the micrographs of specimens. The various of microcracks and fillers could be observed via the comparison of micrographs of aged and virgin specimens.

1.7 Literature review

Various types of silicone adhesives have been created and studied for decades, especially degradation due to aging. Adrian *et al.* (Antosik, 2018) investigated the behavior of silicone pressure-sensitive adhesives, which have been aged at 20°C and 70°C. Aging periods have been discretely distributed from 1 day to 92 days. The shrinkage increased at the beginning and then became stable. Adhesion of silicone films has not been changed by thermal aging. Silicone foaming as a sealant for bridge joints has been investigated by Ramesh *et al.* (Malla, 2011), focusing on degradation due to thermal aging. High temperature, 70 °C, caused the increase of modulus of sealants tensile tests, which was also presented in the aging at low temperature, -36°C. Besides, the aging of temperature cycles between -29°C to 24°C has been conducted, which induced the decrease of tensile stress and strain but didn't change the moduli of aged silicone sealants. Hydrothermal aging analysis of silicone adhesive has been conducted by Jue *et al.* (Li J. a.-K., 2012). 85 °C and 85% RH (relative humidity) has been implemented to silicone adhesives from 25hr up to 300 hrs. It has been concluded that the hydrogen bond was responsible for adhesions of materials. Plasticization could break hydrogen bonds to reduce materials adhesion. But the reduction of adhesion was capable of being recovered by the elimination of moisture from interfaces. Structural silicone adhesive aged in elevated temperature and humidity,

explored by Sun et al. (Sun, 2018). The study concluded that the hardness and tensile strength reduced during aging. In the meanwhile, elongation increased, which was interpreted by changes in internal molecular chains. Likewise, the deterioration of interfaces of silicone adhesive and glass is more severe than the degradation of materials itself. Carlos (Montemayor, 2014) studied the thermal aging of silicone adhesives at very high temperatures, including 200 °C, 225 °C, 250 °C, 275 °C, and 300°C. Elongation, as the fastest degraded property, has been discovered in the aging process, which was attributed to the chemical changes, such as oxidation, hydrolysis—those chemical changes directly reflected in the physical properties, including elongation. Moreover, moisture with various pH value has been considered as an important impact in the study of Ramesh *et al.* (Keshavaraj R. a., 1993). Acid solutions (pH = 3) and alkaline solutions (pH = 11) would impel silicone adhesives increase the cross-link density. However, the prolonged aging process will degrade the mechanical properties due to changes in cross-link density.

Silicone adhesives have been applied in various industries but have not been fully studied the influence of hydrolytic aging. The procedure of degradation has not been explored as the time and temperature increased. In addition, the alteration of cross-link density has been mentioned by the researcher, but detailed structural change has not been studied.

2 CHAPTER 2: Materials and Methods

2.1 Experimental design

This research aims to study the degradation mechanism and characterization of silicone adhesives subjected to hydrolytic aging. In addition, accelerated aging tests has been done under short-span controlled lab conditions. 60°C, 80°C, and 95°C are utilized as the temperatures for accelerated aging within desalinated water and salinated water spanning up to 30 days. Moisture absorption ratio, tensile failure, and cyclic tests were performed on aged specimens to investigate the deterioration of mechanical properties. FT-IR spectroscopy would be utilized to capture the various vibration of functional groups on the adhesive chains, and thus judge the chemical changes of hydrolytic aging. DMA could gain curves of storage modulus E' , loss modulus E'' and $\tan \delta$, the ratio of loss modulus to storage modulus E''/E' . Three curves provide three approaches to calculate T_g to evaluate the plasticization or crystallization based on the comparison of T_g for aged and unaged specimens. SEM is an effective technique to detect the micro-cracks induced by accelerated hydrolytic aging.

2.2 Sample preparation

A PDMS-based adhesive was selected in this study. This adhesive possesses a paste form before application and solidifies after curing at room temperature. The sticky adhesive was cast into a customized mold with 20 samples for each plane shown in Figure 2.1. Immediately, the extra adhesive above the surface of mold was disposed of by a wood stick to ensure each sample matched the standard dimensions in Figure 2.2 mentioned in ASTM D412 (Die C) (D412, 2006). Adhesive specimens were cured for 7 days in room conditions ($22\pm 2^\circ\text{C}$, $50\pm 3\%\text{RH}$) then were cast.

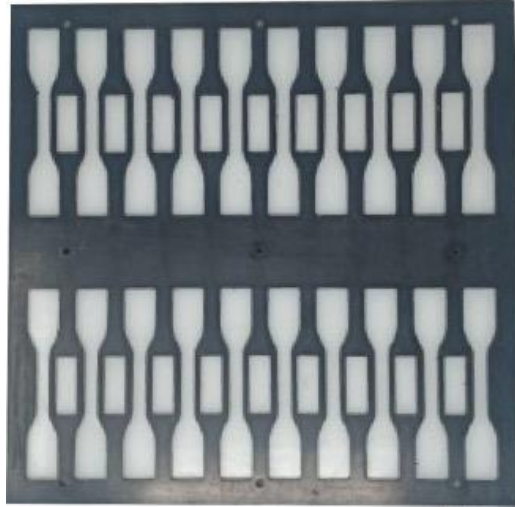


Figure 2.1 Mold for sample preparation

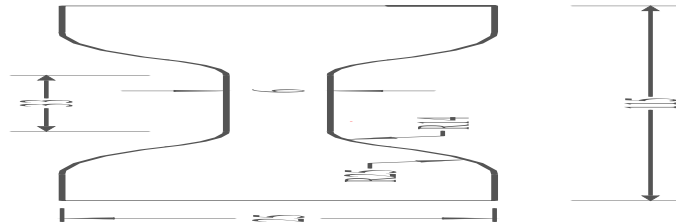


Figure 2.2 Standard dimension for dog-bone samples

2.3 Accelerated hydrolytic aging

As the aging of materials in real life may take years or even decades, accelerated aging tests have been used in this study. In order to simulate weather conditions without time-consuming aging, hydrolytic aging at elevated temperatures, 60°C, 80°C and 95°C, were applied for accelerated aging. In this regard, desalinated water was operated by distilled water with pH = 7 to simulate high-humidity environments. Salinated water was applied by artificial seawater, the sea-salt solution with pH = 8.2, based on ASTM D1141-98 (D1141-98, 2008), to imitate marine environments. Desired periods of aging were 1 day, 10 days and 30 days to investigate time influences for specimens under hydrolytic aging at elevated temperatures. The time-temperature superposition would implement a diverse level of deterioration of samples via desalinated and

salinated water. 10 specimens were immersed in solutions in sealed containers to maintain constant pressure. Grid guards were placed under the specimens to make sure that the specimens are exposed to the conditions from all sides evenly Figure 2.3. Samples were aged in ovens in the absence of light so that UV elements could be excluded from impacting the degradation of materials.

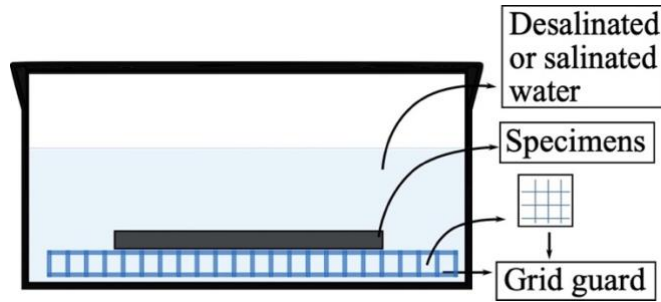


Figure 2.3 A schematic container to display immersion situation.

2.4 Water uptake

Before submerging, the weight of each specimen was measured and recorded using an electronic scale with a precision of 0.0001g. At desired aging times, samples were removed from containers and immediately blotted with tissue paper; after that, measurements of weight were taken on the same scale. In this regard, the percentage of water uptake can be written as

$$\text{Water uptake (\%)} = \frac{W_t - W_0}{W_0} \times 100 ,$$

where W_t and W_0 are weights of samples after desired immersion and before immersion, respectively.

2.5 Mechanical tests

A uni-axial universal Testing Machine (TestRecources 311 Series Frame) was used for quasi-static tensile tests. The tensile machine is equipped with a pair of roller grip (D412, 2006), shown in Figure 2.4, which effectively impede the slippage of silicone adhesives during testing.

All tests were displacement controlled with a crosshead speed of 50mm/min. The distance between the extensometer grips was set to 1 inch, and all the experiments were performed at room conditions ($22\pm 2^{\circ}\text{C}$, $50\pm 3\% \text{RH}$). Each test has been repeated with 5 samples for reliability control. Tensile strength, elongation at break and elastic behaviors exhibit the deterioration of mechanical properties after accelerated hydrolytic aging. In monotonic failure tests, the samples

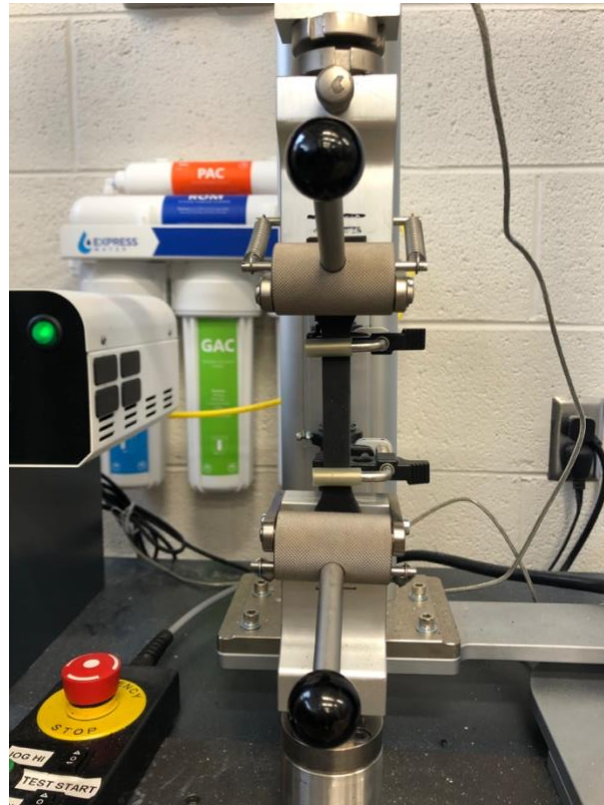


Figure 2.4 Tensile machine with roller grips.

were stretched until breakage while in the cyclic test, the samples were stretched to preset amplitudes of 25%, 50%, 75% and 90% of elongation at the breakpoint of virgin samples, corresponding to the strain of 87%, 174%, 262%, and 314%, respectively. Due to aging damage, aged specimens might break before completing the fourth cycle. Each monotonic cyclic test for one aging condition has been repeated 3 times for reliability control. Each sample is subjected to a non-relaxing cyclic test with increasing amplitude, where the samples are loaded one time at

each amplitude in accordance with Figure 2.5. In the course of deformation, elongation of the central zone of 1 inch has been measured by an external extensometer. The cyclic experiment is designed to illustrate the evolution of the permanent set and stress softening during the primary loading for both unaged and aged samples.

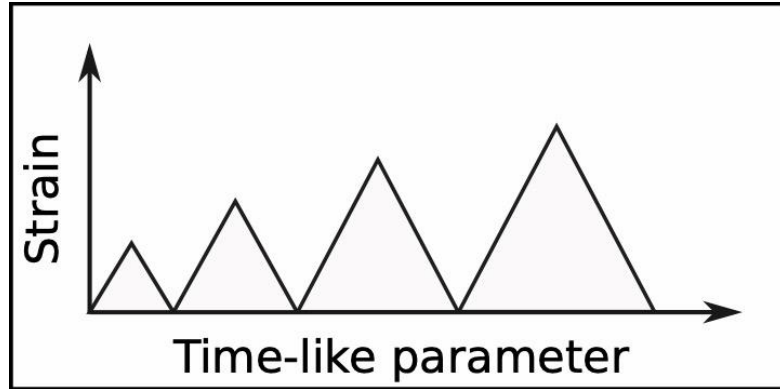


Figure 2.5 A schematic curve for cyclic test

2.6 FT-IR

Various aging conditions inducing chemical alterations could be detected by FT-IR Spectroscopy on the specimen's surface. The functional groups of chains would be denoted in the spectra of FT-IR. One sample per condition tested by using Jasco FT/IR - 4600 spectrometer,



Figure 2.6 Jasco FT/IR - 4600 spectrometer.

spectra was detected from 4000 to 400 cm^{-1} at a resolution of 4 cm^{-1} and an accumulation of 64. The angle of the incident was set at 45° with the monolithic diamond as the ATR prism.

2.7 DMA

Rectangular specimens ($35\text{mm} \times 12\text{mm} \times 3\text{mm}$) were customized and immersed into desalinated water and salinated water for 1 day, 10 days, and 30 days. After carrying out the visual inspection, one of the aged samples from each condition was selected and tested. Single cantilever tests were performed on the TA Instrument DMA Q800 machine shown in Figure 2.7 from -150°C to -70°C with a speed of 3°C per min. The test has been performed in the linear

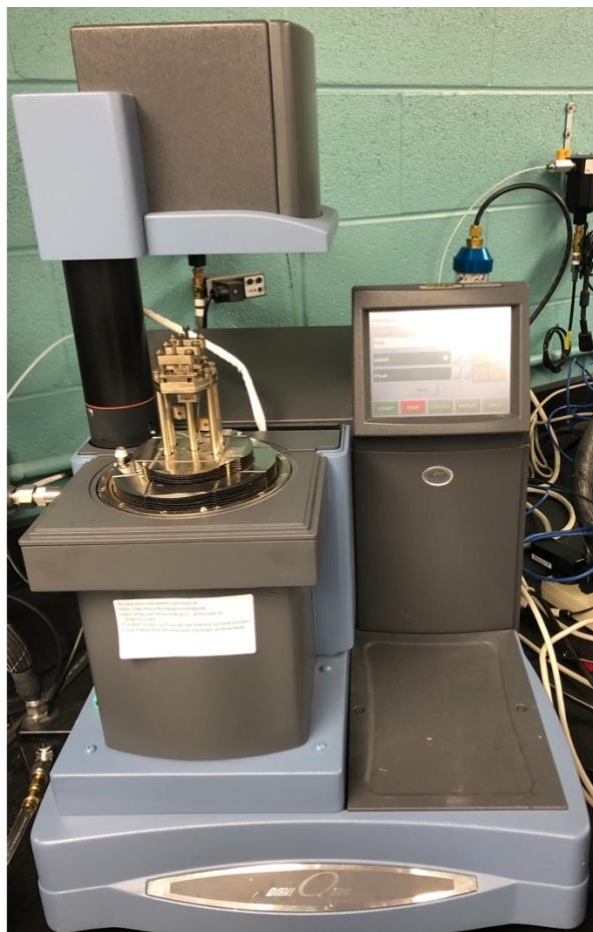


Figure 2.7 TA Instrument DMA Q800 machine.

viscoelastic region (LVR) using a strain amplitude of $15\mu\text{m}$ and a frequency of 1.0 Hz . The machine will derive the stress-strain results, which are used to calculate storage modulus, loss

modulus and $\tan \delta$. These curves evaluate the chain mobility and shape resilience of cyclic deformation. Another imperative parameter could be obtained is, which is relevant to cross-link density and chains free volume.

2.8 SEM

Morphology of virgin and 30-day immersed specimens was inspected by a scanning electron microscope (Zeiss EVO LS 25) with an accelerating voltage of 3.0kV. Desalinated and salinated water aging for 30 days were gauged by various micro-graphs on the tensile fracture surfaces of specimens.

3 Chapter 3: Test Results and Discussion

3.1 Water uptake

Figure 3.1 shows that water absorption within dispartage solutions versus the square root of duration. There is no doubt that desalinated water provides an environment that allows materials to absorb more water, especially under high temperatures and long durations. On the contrary, salinated water led to a slight decline and then increased weight in 60°C, which is completely opposite to 80°C and 95°C. In desalinated water, a mild environment, the voids of specimens were filled with water, thus causing so-called swelling. Time-temperature superposition promotes the process of water absorption, especially in 95°C 30-day aged specimens with 17.77% weight gain. However, sea salt from salinated water could prevent the penetration of water into materials, which is also mentioned by Firas *et al.* (Awaja, Cracks, microcracks and fracture in polymer structures: Formation, detection, autonomic repair, 2016). At 60°C, comparatively low temperature in this study, specimens gain weight of 0.06% for 30 days, which results from the salt barrier. As temperature rises, 1-day and 10-day aging-induced a slight weight gain, which proves that high temperatures might break the barriers between

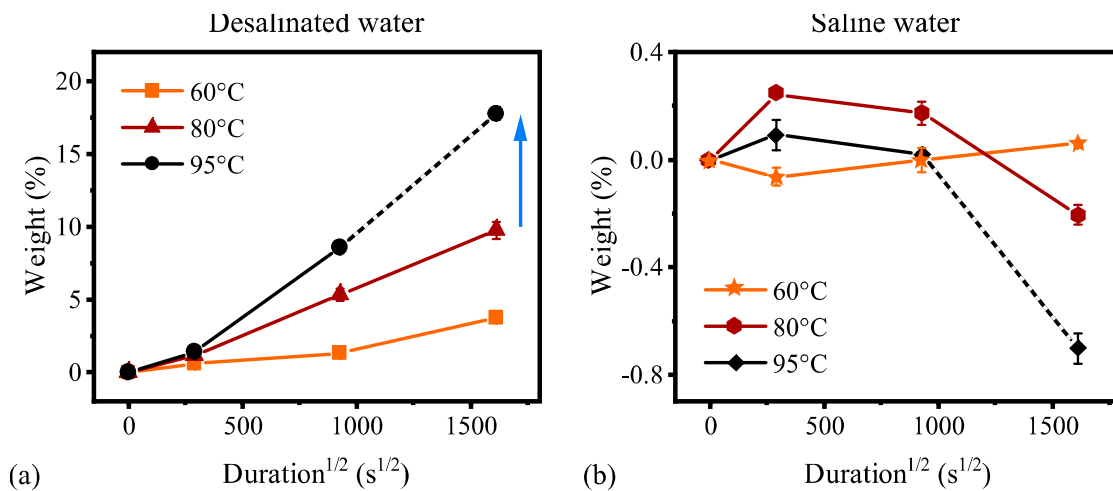


Figure 3.1 Water uptake under temperature superposition for (a) desalinated water and (b) salinated water.

solutions and samples, especially in 80°C. 95°C started to cause damage inside samples; and thus, water cannot be massively absorbed by materials. In addition, chemical compounds in the medium of salinated water, such as sodium chloride, with higher pH are likely to generate chemical reactions with specimens, and then cause chain scissions, followed by leaching. The sea-salt barrier and leaching process caused 0.7% weight loss of 95°C 30-day aged specimens.

In summary, the desalinated water and salinated water created disparate deterioration mechanisms on PDMS-based adhesive.

3.2 Mechanical properties

3.2.1 Tensile failure tests

The variation of the tensile strength, as well as elongation at break versus temperature in the case of desalinated water, are given in Figure 3.2. Regarding submerging in desalinated water, aging with gradually rising temperatures impels descending tensile strength, while initially increasing and later-on declining elongation at

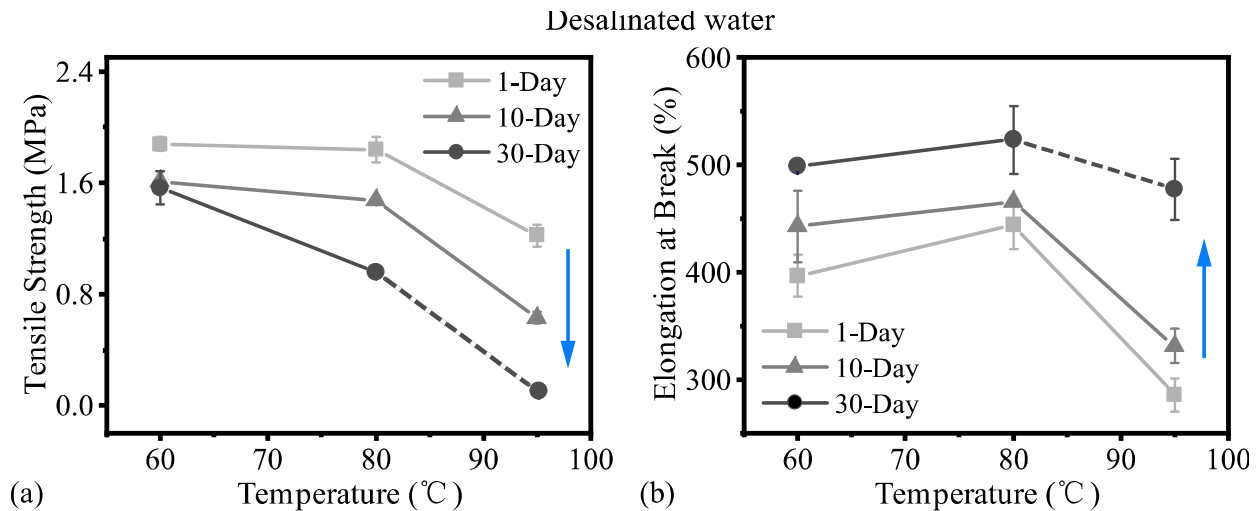


Figure 3.2 Temperature comparison for (a) tensile strength and (b) elongation at break of samples submerged within desalinated water.

break. No matter how long the aging duration is, elongation at break under 80°C-aging arrives pinnacle. Nevertheless, 95°C is high enough for aged samples to degrade in tensile strength and elongation at break acutely.

On the other hand, what is displayed in the duration comparison shown in Figure 3.3 is that tensile strength and elongation at break ascend and descend, respectively. Tensile strength is shown in Figure 3.3(a) rising at 60°C and 80°C 1-day aging was triggered by the physical cross-linking of chains due to the appropriate temperature. For further long-term aging, tensile strength declined to a different extent. Tensile strength is an inverse ratio to the square root of aging duration at 95°C. Elongation at break, exhibited in Figure 3.3(b), increased under 60°C and 80°C. As aforementioned, 95°C inhibited continual growth of elongation at break that would have increased on 1-day and 10-day aging. But 30-day aging displayed sharp increasing elongation at break as a result of plasticization. Water as a plasticizer is able to cause structural changes in silicone adhesive under long-term aging.

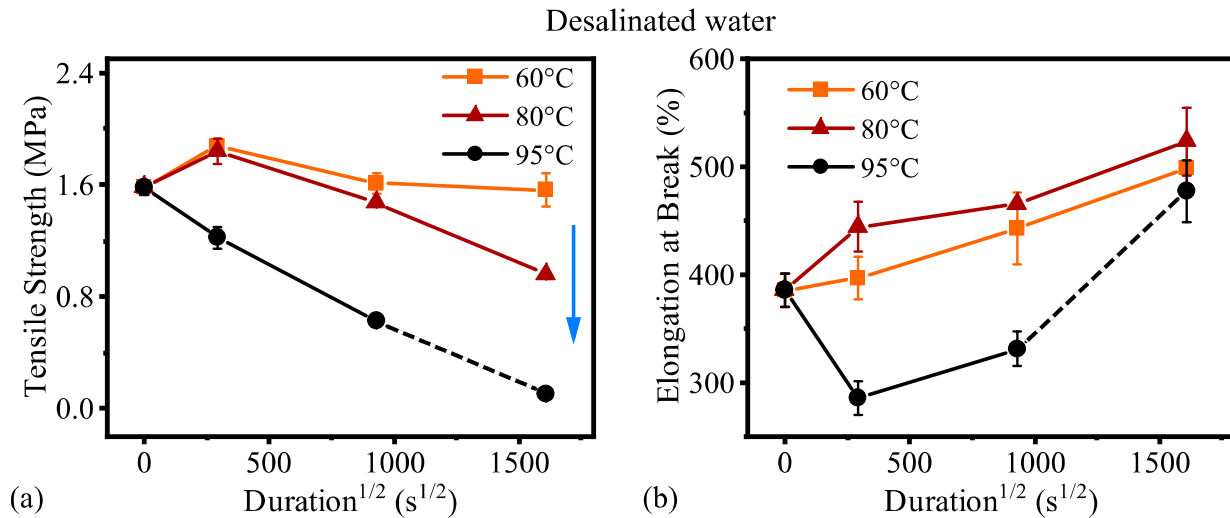


Figure 3.3 Duration comparison for (a) tensile strength and (b) elongation at break with immersion of desalinated water.

Figure 3.4 places the variation of tensile strength and elongation at break as a function of temperatures under the immersion condition of salinated water. There is no doubt that tensile strength decreased from 60°C to 95°C shown in Figure 3.4(a). Regarding submerging into salinated water, elongation at break generally exhibits an increasing trend in Figure 3.4(b), except for 1-day aged specimens from 60°C to 80°C. Similarly, elevated temperature could cause decay of tensile strength and rising elongation at break within salinated water.

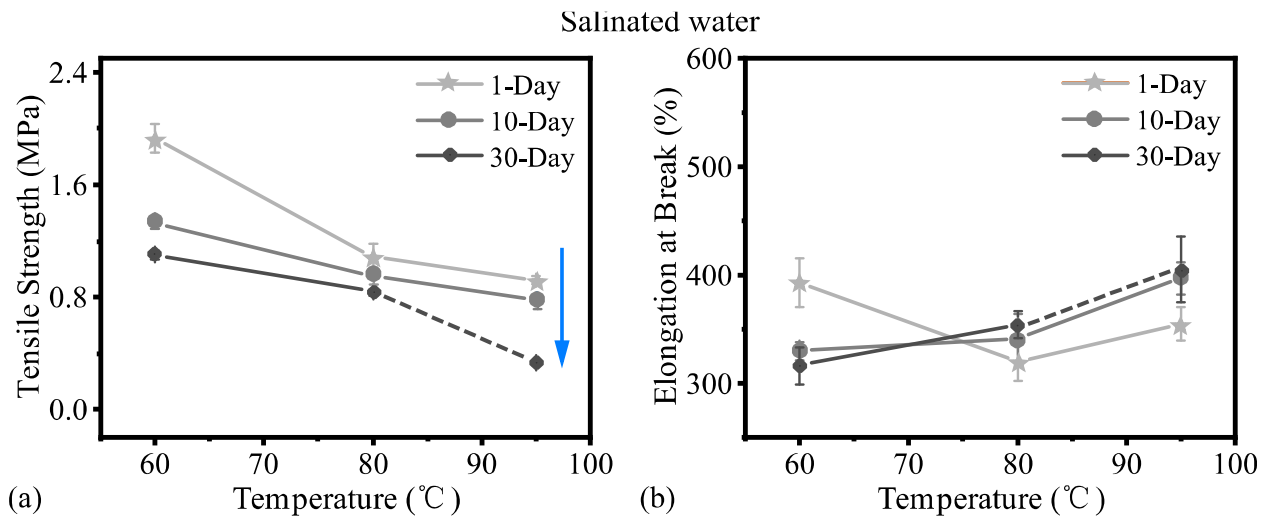


Figure 3.4 Temperature comparison for (a) tensile strength and (b) elongation at break within salinated water.

The evolution of tensile strength and elongation at break versus square root of time shows in Figure 3.5. As time passed, tensile strength declined after the desired aging process, which embodied in Figure 3.5(a). But, 60°C 1-day aging causes the increasing tensile strength of specimens. Alteration of elongation at break exhibits in Figure 3.5(b). Lengthened elongation at

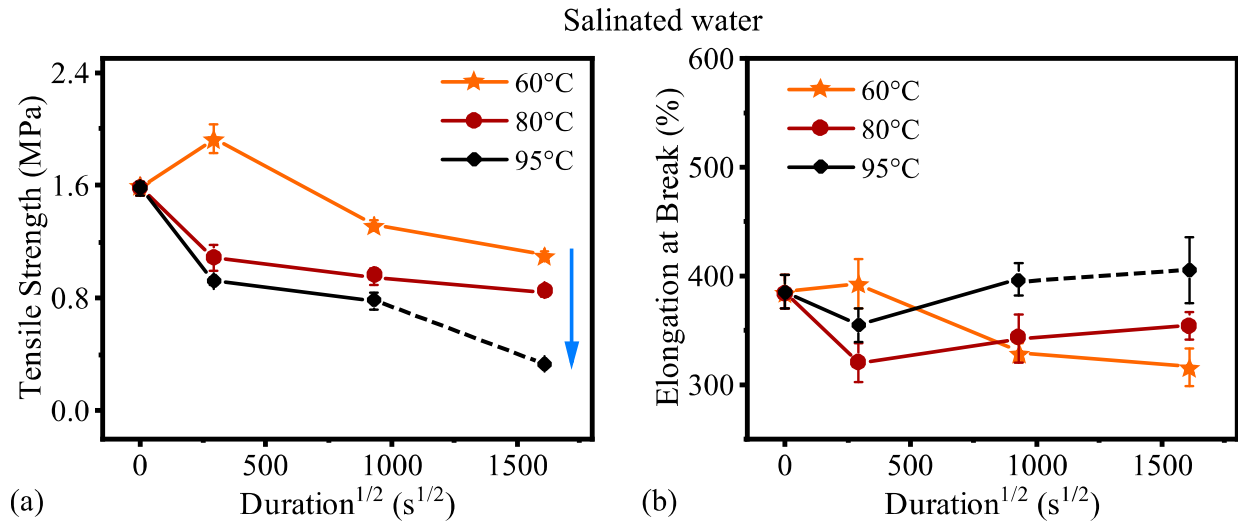


Figure 3.5 Duration comparison for (a) tensile strength and (b) elongation at break within salinated water.

break of specimens after 80°C and 95°C 30-day aging is opposite to reduction in 60°C 30-day aging. In 1-day aging, 60°C was conducive to increase the elongation at break of specimens, which is completely different in 80°C and 95°C.

Desalinated and salinated water at 60°C exerted an identical impact on materials after 1-day of aging in both tensile strengths shown in Figure 3.6 (a) and elongation at break Figure

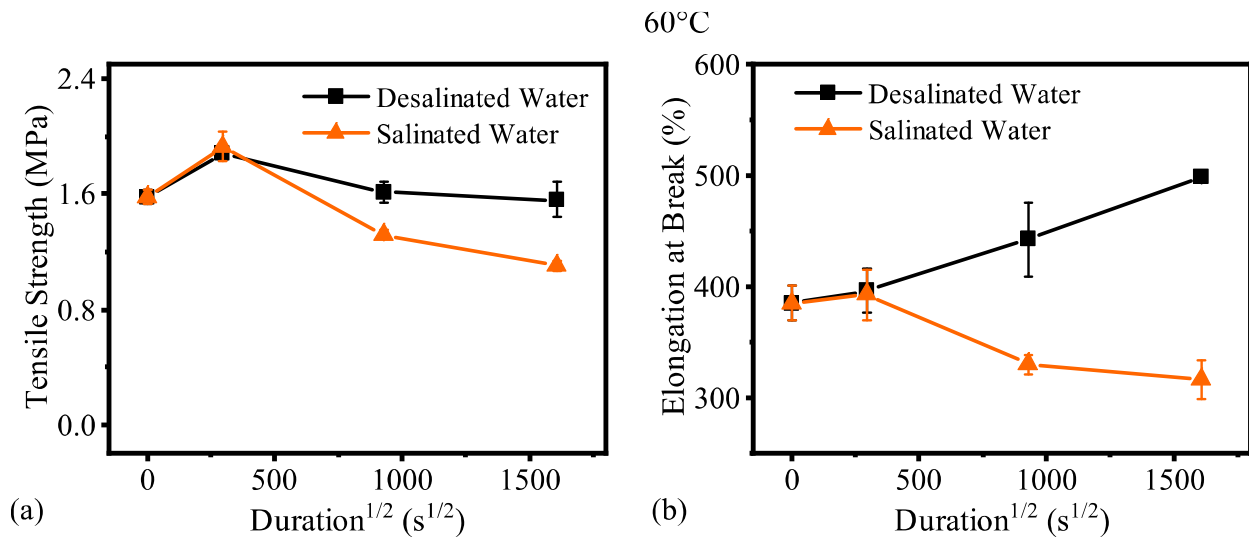


Figure 3.6 Comparison between influence of desalinated and salinated water on specimens of (a) tensile strength and (b) elongation at break at 60°C.

3.6(b). Afterward, when tensile strength was reduced in both environments, descending elongation at break happened after specimens were immersed in salinated water, in contrast with the distilled water. Salinated water caused more damage to silicone adhesives within the inferior of tensile strength and elongation at break than desalinated water. Higher pH value and sea salt barrier might act on adhesive specimens to generate such a variety of degradation between two immersion mediums.

Synergized of aging durations and temperature at 80°C shows in Figure 3.7 to compare the mediums of desalinated and salinated water. In Figure 3.7(a), tensile strength increased for 1-day aging within desalinated water. After that, tensile strength decreased in desalinate water the same as in salinated water-finally, tensile strength is shown in slight differentiation between them. As for Figure 3.7(b), desalinated water facilitated increasing elongation at break as opposition to salinated water. In total, specimens submerged within salinated water for 1 day might involve in an equilibrium. The variation of tensile strength and elongation at break of specimens induced by salinated-water is minor than by desalinated-water for long term aging.

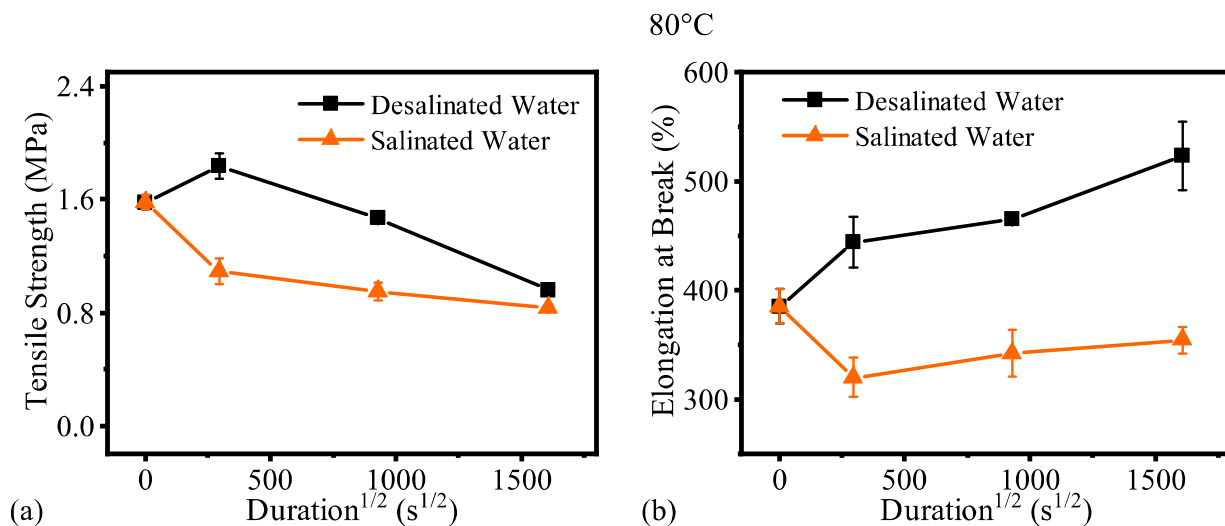


Figure 3.7 Comparison between influence of desalinated and salinated water on specimens of (a) tensile strength and (b) elongation at break at 80°C.

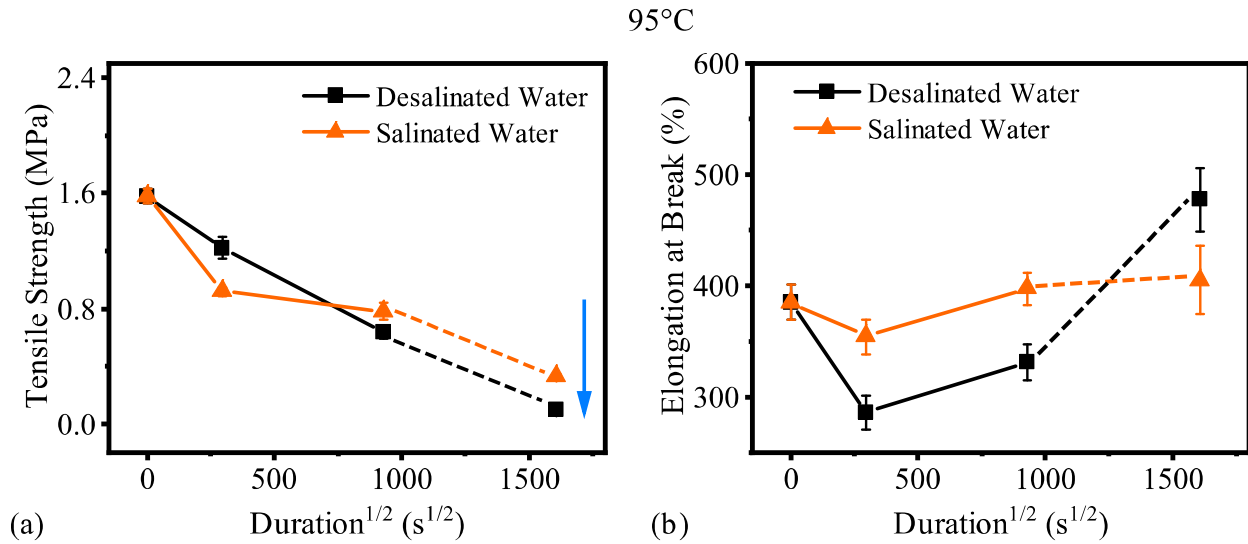


Figure 3.8 Comparison between influence of desalinated and salinated water on specimens of (a) tensile strength and (b) elongation at break at 95°C.

Contrasting the desalinated water and salinated water at 95°C is in Figure 3.8. Tensile strength is shown in Figure 3.8(a) declined in desalinated and salinated water, which proved the destructive impact on 95°C synergized by prolonged durations. Similarly, elongation at break sharply dropped in desalinated water for 1 day and 10 days immersion, which displayed in Figure 3.8(b). Afterward, swiftly increasing elongation at break happened. However, elongation at break of specimens after salinated water aging changed slightly. Salinated water might protect specimens from a serious loss of mechanical properties.

Conclusively, under 60°C, salinated water inducing degradation of silicone adhesive was more severe than desalinated water, which might attribute to higher pH value. At 80°C, specimens after 1-day immersion of salinated water degraded in mechanical properties, which was diverged from specimens after 1-day immersion of desalinated water. The prolonged aging process accelerated the degradation of specimens aged by desalinated water but not by salinated water. 95°C caused further damage to silicone adhesive submerged not only in desalinated water

but also within salinated water. But, salinated water was conducive to generate chemical reactions to create new crosslinks, which lessened the degradation by high temperatures.

The tensile behavior of the virgin and aged specimens showed in Figure 3.9. Specimens performed elastic behaviors, in spite of specimens degraded by various aging conditions. When they were subjected to desalinated water at 60°C and 80°C for 1 day, specimens displayed increasing ductility with hardening behaviors (Deroine, 2014). At the same degree, prolonged aging durations impelled specimens to ascend their ductility and decrease their load sustainability, named softening behaviors. Specimens exhibited brittle behaviors after 95°C 1-day and 10-days aging. Especially, for immersion of 95°C at 30-days, specimen barely sustain load but had eminent ductility. What exhibits in salinated-water immersion results is that only 60°C 1-day compelled specimens to be more hardening. Brittle behaviors showed after aging of 60°C 10-day, 30-day, and immersion at 80°C simultaneously at 95°C 1-day and 10-day. 95°C 30-day aging caused specimens to be more stretchable and less sustainable load.

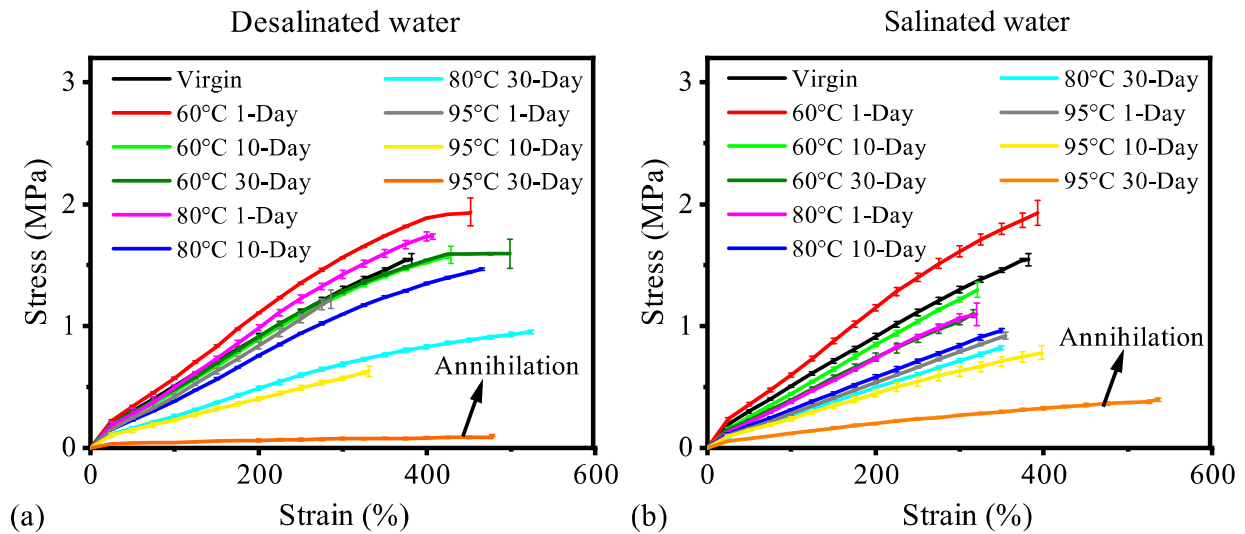


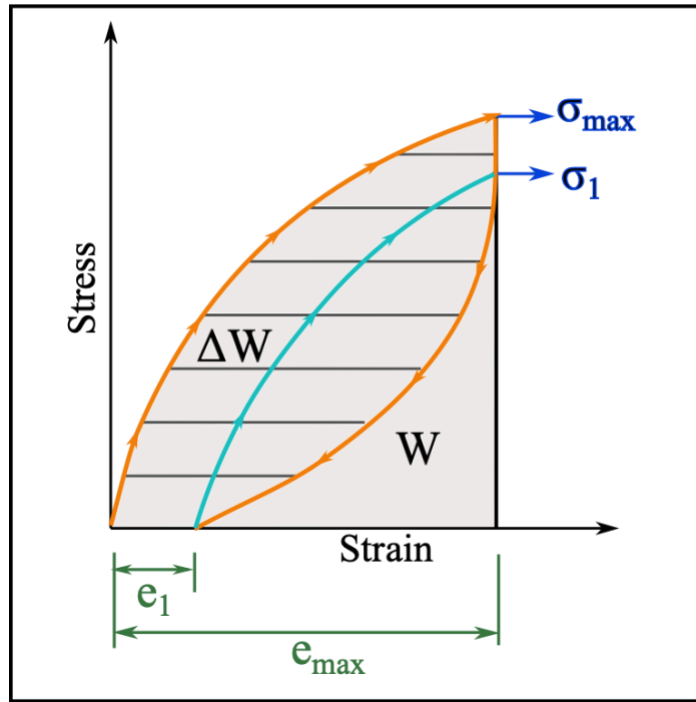
Figure 3.9 The stress-strain curves of specimens for (a) desalinated water and (b) salinated water.

3.2.2 Tensile cyclic tests

To gain a comprehensive knowledge of the effects of hydrolytic aging on silicone adhesive, aged specimens characterized various inelastic behaviors by cyclic tensile tests where specimens are confined by certain displacements under cyclic loading-unloading conditions. Stress softening is shown as σ_1 for the reloading phase, which is lower than σ_{max} , the maximum stress for the first loading. Specimens undergo loading-unloading condition and cannot immediately reverse back to the initial strain, so-called residual strain e_1 in Figure 3.10(a). Besides, hysteresis is the area of loading-unloading curves, which is ΔW exhibited in Figure 3.10(a). Therefore, relative stress softening σ^* , relative residual strain e^* , and hysteresis loss W^* are utilized to eliminate the effect conducted by assigned strain for each cycle in an attempt to study the combination of degradation mechanism of damage induced by deformations and various environmental conditions.

The stress-strain curve of the cyclic test of virgin material has been shown in Figure 3.10(b). The stress softening is observed over the course of reloading, only if the loading occurred and rearranged the polymer chains to the desired strain. The phenomena of hysteresis and residual strain can be discerned from Figure 3.10(b). It is clarified that different strain levels could differentiate the values of stress softening, residual strain, and hysteresis, which depends on the degree of rearrangement of fillers and polymer chains. Those inelastic characteristics increase as the desired strain grows. Therefore, in an attempt to eliminate the influence of the strain value, the relative value is selected to investigate the damage induced by cyclic deformation.

(a)



(b)

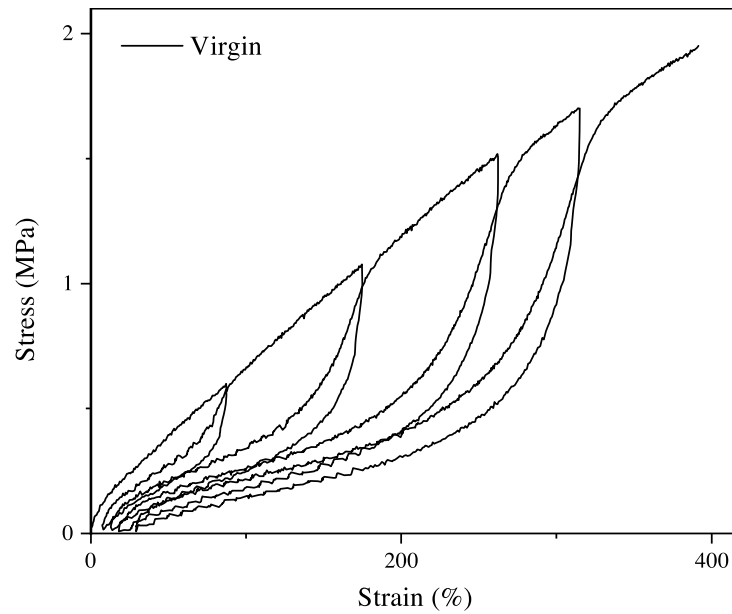


Figure 3.10 (a) Schematic representations for relative stress softening, relative residual strain and hysteresis loss and (b) Stress-strain curve of cyclic tensile test of virgin specimens.

Firstly, relative stress softening σ^* is defined as the ratio of the stresses at the maximum strain of the second cycle σ_1 (see Figure 3.10(a)) to the stress at the same strain value of the first cycle σ_{max} (i.e. $\sigma^* = \sigma_1/\sigma_{max}$) both referred to the same aging condition. The relative stress softening has been altered by hydrolytic aging within neither desalinated water (see Figure

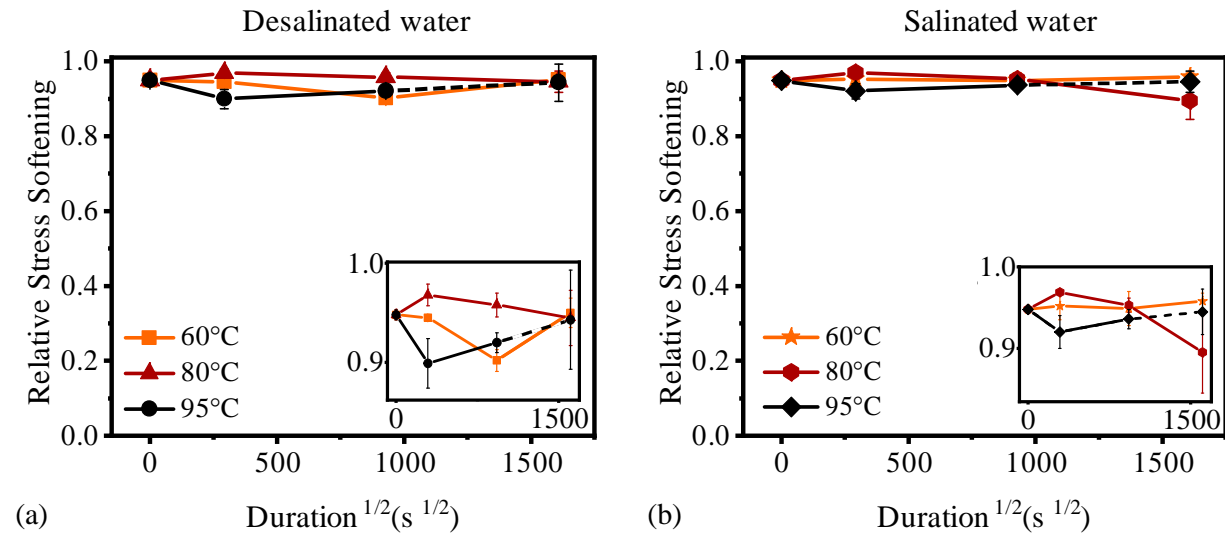


Figure 3.11 Relative stress softening for (a) desalinated water, and (b) salinated water in 87% strain.

3.11(a)) nor salinated water (see Figure 3.11(b)) at the strain of 87%. In other words, the relative stress softening is the stress comparison between loading and reloading periods. During loading, fillers would be oriented along with applied force and entangle with polymer chains. After that, the entanglements prevent the fillers from retracting fully to the initial state due to the presence of knots (Gao, 2015). When reloading presents, less stress value is required to re-orient and re-entangle fillers and polymer chains. Hydrolytic aging under intense heat scarcely influenced the ratio of the reloading stress to the loading stress in the 87% strain. The variation of relative stress softening of specimens aging for 1 day might present the influence of temperatures. 60°C aging basically keeps the relative stress softening of aged specimens as a constant, whereas 80°C might increase the cross-link density, which is conducive to bounce back for the materials during

releasing periods. Thus, materials demand higher stress to re-orient the fillers and polymer chains through reloading. Nevertheless, 95°C caused a different degradation mechanism to decline relative stress softening.

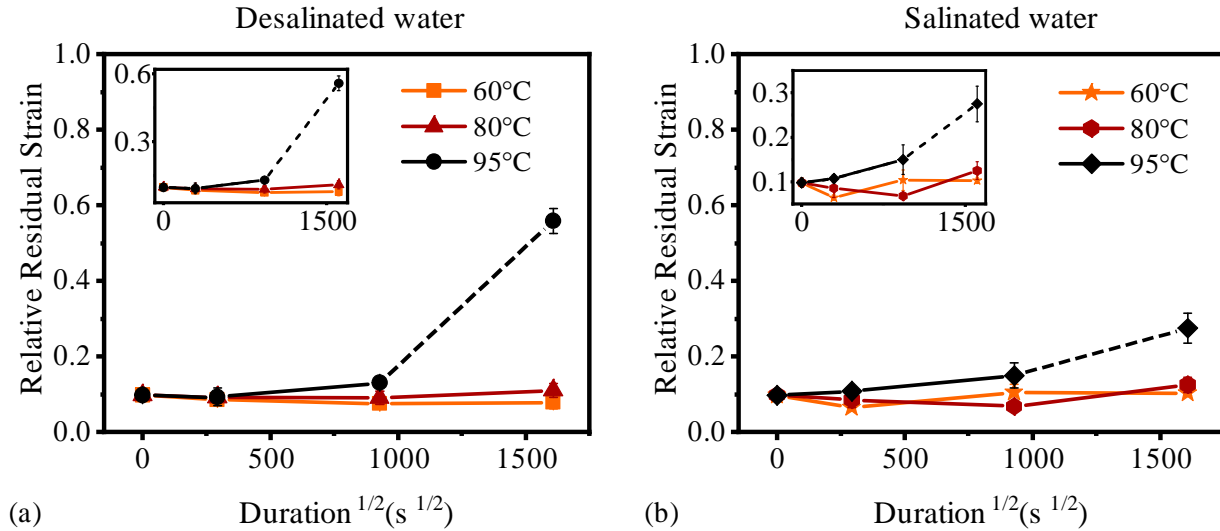


Figure 3.12 Relative residual strain for (a) desalinated water, and (b) salinated water in 87% strain..

Secondly, relative residual strain e^* can be interpreted by residual strain after the first cycle e_1 (see Figure 3.10(a)) over the maximum strain e_{max} (i.e. $e^* = e_1/e_{max}$). For specimens submerged within various solutions, the temperatures 60°C and 80°C in both desalinated and salinated water were not able to exert overt changes of material properties (see Figure 3.12). In addition, what shows in the enlarged graph is a marginally decrease of relative residual strain after hydrolytic aging at 60°C and 80°C. The appropriate temperatures could reduce residual strain, which has been approved by LiHong *et al.* (Huang, 2019). However, the temperature of 95°C, especially in desalinated water, accumulating time effects caused a considerable increment of relative residual strain. As aforementioned, the formation of entanglement during the loading phase, constraints the retraction of fillers, which is depicted in the form of residual strain. The constraints might be derived from friction forces, which are proposed by Xing and Biqiong (Su,

2018). Likewise, the amount of chemical bond reflecting in hysteresis loss would cause the increase of residual strain during the cyclic deformation. Hydrolytic aging at 95°C impelled specimens to generate chemical cross-link, shown in Figure 3.14, which might contribute to impeding the reverse motion of materials. The increasing cross-link density combined with the rapid growth of hysteresis loss shown in Figure 3.13 could cause a substantial increase in residual strain.

Lastly, the relative hysteresis loss W^* is written as the ratio of the dissipated energy in the first cycle, which is depicted in Figure 3.10(a) (i.e. $W^* = \Delta W/W$). In fact, the hysteresis loss reflects how much energy is dissipated during cyclic tensile tests in each aging condition. The variations are shown in hysteresis loss for desalinated water (see Figure 3.13(a)) and salinated water (see Figure 3.13(b)). As shown, hydrolytic aging exerted an impact on specimens to dissipate more energy during cyclic tension. Less orientation of the polymer chains and fillers happened during cyclic loading, which increased the amount of chemical bond breakage. The

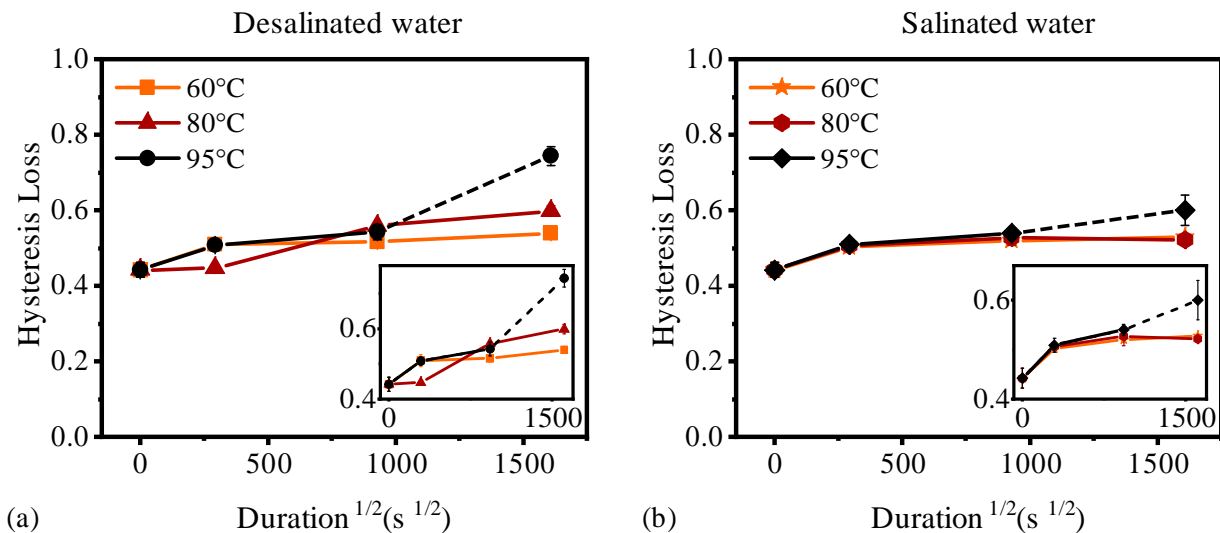


Figure 3.13 Hysteresis loss for (a) desalinated water, and (b) salinated water in 87% strain.

bond breakage cannot recover in a short period, so that hysteresis loss of aged specimens

increased (Su, 2018). Besides, the marginal increment of hysteresis loss at 95°C is a reflection of breaking chemical bonds owing to loss of chain mobility, corresponding to the decreasing peak of $\text{Tan } \delta$ shown in Figure 3.15, which is in agreement with the study of Abd-El *et al.* on filled silicone rubber (Dorfmann, A constitutive model for the Mullins effect with permanent set in particle-reinforced rubber, 2004).

Conclusively, the variations of σ^* , e^* and W^* between virgin and aged specimens are shown in Figure 3.11, 3.12, and 3.13. If the 95°C 30-day aging could be regarded as annihilation, the variation of σ^* , e^* , and W^* between virgin and aged specimens will be within 0.2. In other words, the relative values of stress softening, residual strain, and hysteresis loss eliminated the softening and brittle behaviors induced by hydrolytic aging. However, macro-structural changes induced by hydrolytic aging would merge under loading-unloading conditions. Those environmental alterations combined with the damage caused by cyclic load, which led to slight variation of σ^* , e^* , and W^* .

3.3 FT-IR analysis

Hydrolysis is an aqueous process involving chain scission and therefore leads to alterations of molecular structures (G"opferich, 1996). There is no doubt that FT-IR spectra, as a potent technique, can identify the changes in the chemical structure of virgin specimens through hydrolytic aging. Figure 3.14 shows FT-IR spectra for specimens submerged in desalinated water and salinated water. To better understand the data, Table 1 shows the wavenumbers at the peaks derived from the FT-IR results with their subordinating wave ranges and assignments.

Desalinated water penetrated into silicone adhesive and gradually generated chemical reactions with material molecules (see Figure 3.14(a)). At the wavenumber of 1410 cm^{-1} , in most of the aging conditions, spectra slightly curtailed after desired aging periods under high

temperatures. Yet, 30-day hydrolytic aging with an increment of absorbance could be as a result of re-crosslinking, especially at 95°C. And the intensity increased as temperatures raised, which proved that high temperatures were contributive to the generation of the new cross-link.

Immersion medium with pH = 7 barely caused chemical reactions of silicone adhesive, which is in agreement with the study of Alok *et al.* on silicone rubber (Verma, 2017).

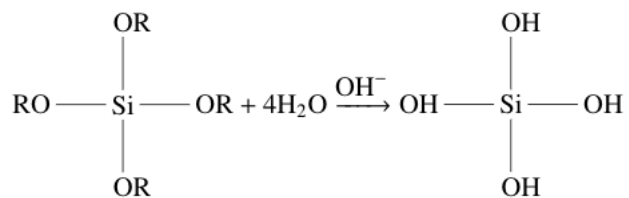
For specimens submerged in salinated water (see Figure 3.14(b)), the peaks at 1410 cm^{-1} exhibit a wider range of intensity than spectra from specimens aged in desalinated water. At this point, adhesives submerged at 95°C for a 1-day period lost a great number of chemical cross-links, which also reflected in the intensity at wave number 1007, 1082, and 2965 cm^{-1} . This reduction caused decreased mechanical behaviors of the materials, including brittle behaviors. Similarly, specimens created new chemical bonds after 30 days aging at 60°C and 80°C, which embodied in the peaks at the wavenumbers of 1577, 1539, 2847, and 2911 cm^{-1} . It is worth mentioning that 80°C 30-day of salinated water impelled the hydrolysis reactions shown in Eq.1, corresponding to the peak at 3386 cm^{-1} related to Si-OH. The band of 2847 cm^{-1} indicates Si-OCH₃ inside of adhesive after aging. The increased quantity of Si-OCH₃ combined with Si-OH generated long chains of materials, shown in Eq. 2, namely, water condensation reaction. Increasing intensity at 1410 cm^{-1} combined with the generation of long chains alleviated tensile properties degradation of specimens that were submerged within salinated water under 95°C for 10 days and 30 days. Likewise, CH₃OH might be leached out, which coincides with scarcely decreasing weights of silicone adhesives. Besides, the escalated intensity at 2911 and 2965 cm^{-1} represents CH Stretching in the methyl group (Lee, 2013). The new structure, named ring skeleton, generated in salinated aging in accordance with the band near 1580 cm^{-1} (Badertscher, 2009).

Overall, less variation of intensity of 1-day and 10-day aged specimens shows in the environment of desalinated water than salinated water. This phenomenon validates the negative effect of higher pH value on silicone adhesives, related to less tensile strength and elongation at break. From this perspective, the increased tensile strength of specimens aged within desalinated water is possibly due to the increased number of physical cross-links. According to Figure 3.14, desalinated water with 7 pH value cannot provide an appropriate environment for silicone adhesive to conduct plenty of chemical reactions, compared to salinated water

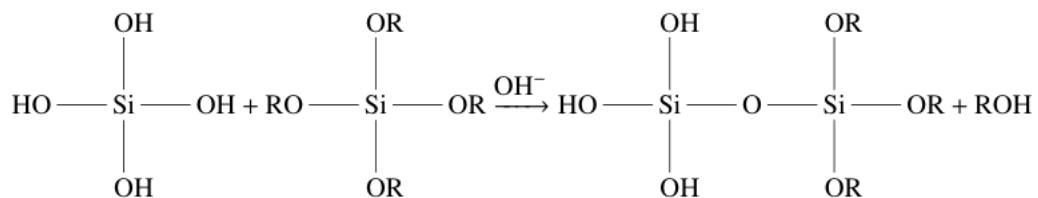
Table 1 Assignments and wave ranges corresponding to FT-IR spectra pinnacles.

Pinnacle in cm^{-1}	Range in cm^{-1}	Assignments
3386	3400-3200	Si-OH (hydrogen-bonded OH)
2965 & 2911	3000-2840	CH _{st}
2847	2840	Si-OCH ₃
1577 & 1539	1610-1550	Ring skeleton
1410	1410	Si-CH=CH ₂
1258	1275-1260	CH ₃
1082 & 1007	1130-1000	Si-O-Si
868	900-800	Si-OH
786	865-750	Si-CH ₃

Equation 1 Hydrolysis reaction.



Equation 2 Water condensation reaction.



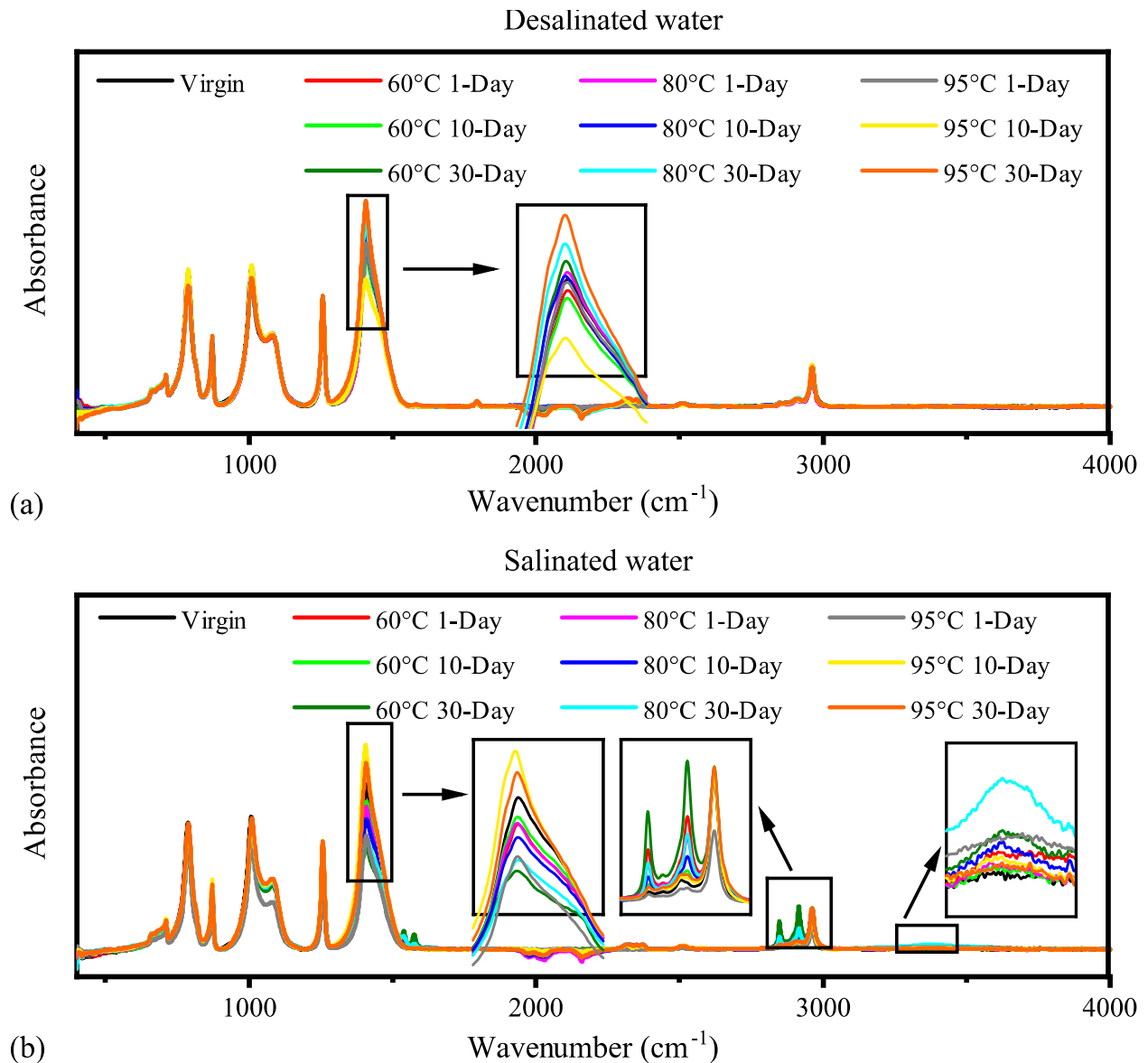


Figure 3.14 The FT-IR spectra of virgin and aged specimens through various durations and temperatures within (a) desalinated water and (b) salinated water.

3.3 DMA analysis

DMA is regarded as a technique to detect molecular motions of rubberlike materials where specimens are applied by a sinusoidal force at a given frequency (Aglan, 2008). Those cyclic deformations would result in stress and strain response of materials calculated by DMA instruments. During the dynamic loading period, the stored energy by polymer molecules is

referred to as storage modulus, exhibiting elastic behaviors of materials. Storage modulus curves embody the materials' stiffness and shape recovery. The rest portion of the energy is relevant to dissipating energy, so-called loss modulus, displaying the viscous characteristics of adhesives, which promises the energy of dissipation via internal motions (Dunson, 2017). Therefore, DMA is utilized to characterize the viscoelastic behaviors of the materials as a function of temperatures to study the stiffness and resiliency of silicone adhesives (Barral, 2000).

Figure 3.15 shows the DMA results of virgin specimens and aged specimens with desalinated and salinated water. The storage modulus E' , the loss modulus E'' and the phase shift $\tan \delta$ of specimens aged in desalinated and salinated water are compared in Figure 3.15 a-f, respectively. Storage modulus curves characterized the transition from glassy to rubbery behavior of materials and obtained glass transition temperature T_g as a significant factor. Loss modulus is defined as the dissipated energy, switched to heat, for each cycle of sinusoidal deformation. The drop of storage modulus of silicone adhesives immersed in desalinated water represents the chain softening, which runs contrary to the study of Barral *et al.* on the thermal aging of TGDDM (Barral, 2000). $\tan \delta$, which reflects the molecular level changes, is the ratio of loss modulus to storage modulus E''/E' .

T_g of virgin and aged specimens was determined by the onset point of storage modulus. The left-shifted onset points of storage modulus represent the reduction of T_g . Meanwhile, the peak of loss modulus and $\tan \delta$, the other manners of measuring T_g , shows shifted left. In general, for the specimens submerged within desalinated water, declining of T_g from -125.28°C to -128.13°C proves the plasticization in materials during hydrolytic aging, which coincides with tensile properties of materials, shown in Figure 3.16. Desalinated water under elevated temperatures permeated into silicone adhesives, which results in increasing the free volume of

molecular chains (Borek, 1998). The Free volume of chains relates to the friction force and required energy during chain motions. Free volume enlarged by water molecules could impel adhesives with a loose internal structure and provide chains with more rotational freedom (Dunson, 2017). The water content of samples can affect their thermo-mechanical properties, and the variation of T_g is associated with changes in the microstructure of the adhesive. Hence, aging under elevated temperatures results in the promotion of water absorption and, consequently, reduction of T_g , displayed in Figure 3.16(a). Table 2 summarized the values of T_g and water content for various aging conditions within desalinated water.

In salinated water aging, 10-day aged specimens at temperatures 80°C and 95°C possess higher T_g than 1-day aged in Figure 3.16 (b). Another approach to influence the T_g of materials is the cross-link density. The increasing number of cross-link would cause the increment of friction force and its required energy during cyclic deformation (Hagen, 1996). As aforementioned, salinated water provided an appropriate environment for PDMS-based adhesives to generate new cross-links, which exerted a profound influence on increasing T_g . Overall, T_g emerges a downward trend for salinated-water aged specimens as a shred of evidence for plasticization.

Hydrolytic aging at elevated temperatures induced the plasticization of silicone adhesives, which varied the visco-elastic behaviors. However, such an aging process is perplexing that the degradation of materials contains several mechanisms. Plasticization is one of the degradation mechanisms, but the abrupt drop of storage modulus and loss modulus of specimens submerged in salinated water at 80°C for a 10-day period has not been exhaustively understood. The degradation mechanism of this special condition would be studied in the future.

Table 2 The water uptake and T_g of specimens for desalinated water under various temperatures.

Aging condition	Square root of time ($s^{1/2}$)	Water uptake (%)	$T_g(^{\circ}C)$
60°C & Desalinated water	0	0	-125.28
	294	0.61 ± 0.045	-126.62
	930	1.32 ± 0.253	-126.96
	1610	3.72 ± 0.223	-127.08
80°C & Desalinated water	0	0	-125.28
	294	1.19 ± 0.024	-126.53
	930	5.36 ± 0.427	-127.04
	1610	9.74 ± 0.585	-127.48
95°C & Desalinated water	0	0	-125.28
	294	1.39 ± 0.075	-126.95
	930	8.54 ± 0.202	-127.49
	1610	17.58 ± 0.452	-128.13

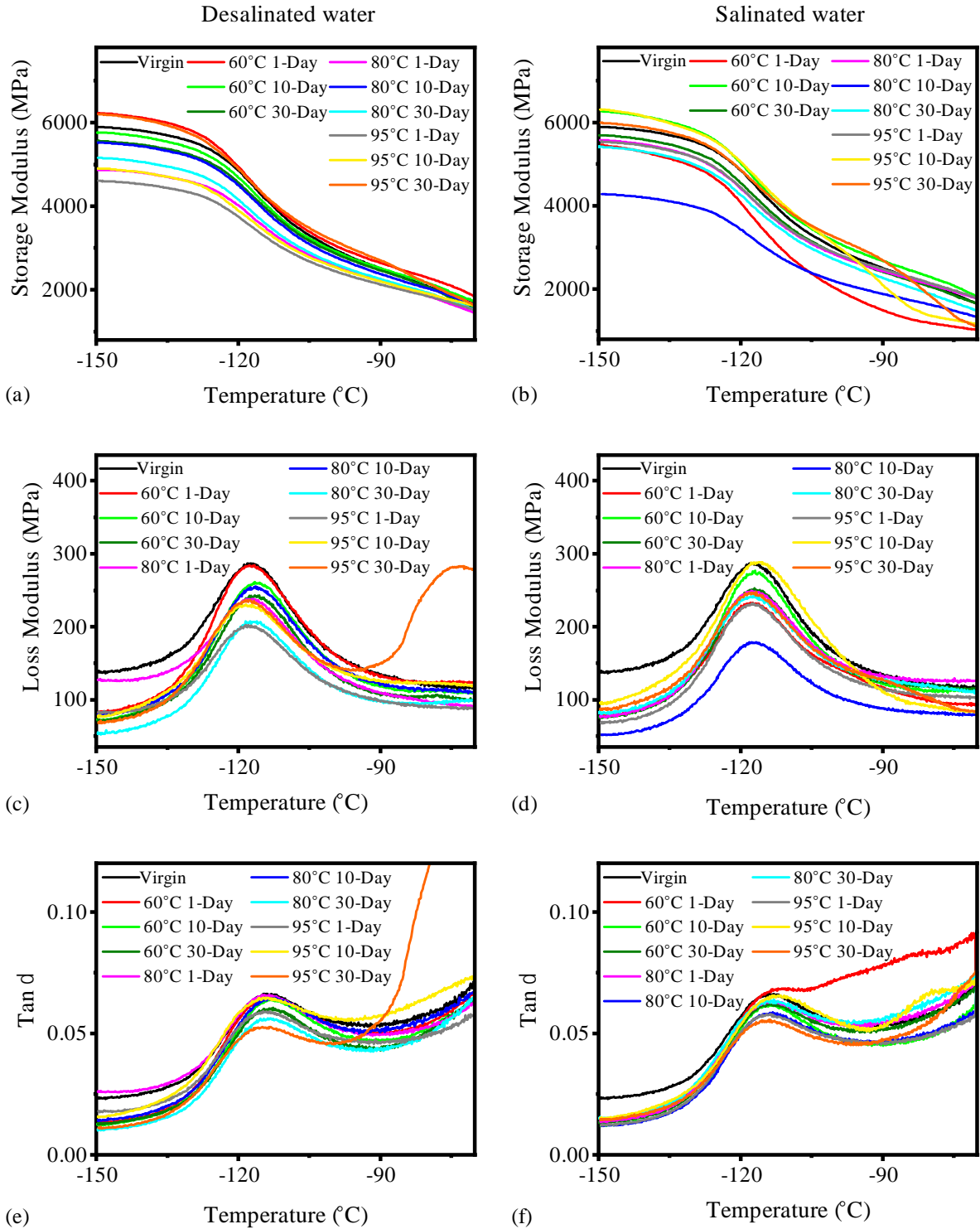


Figure 3.15 Storage modulus variation aged within (a)desalinated water and (b) salinated water, loss modulus changes of (c) desalinated water and (d) salinated water and Tan δ changed due to (e)desalinated water and (f) salinated water aging.

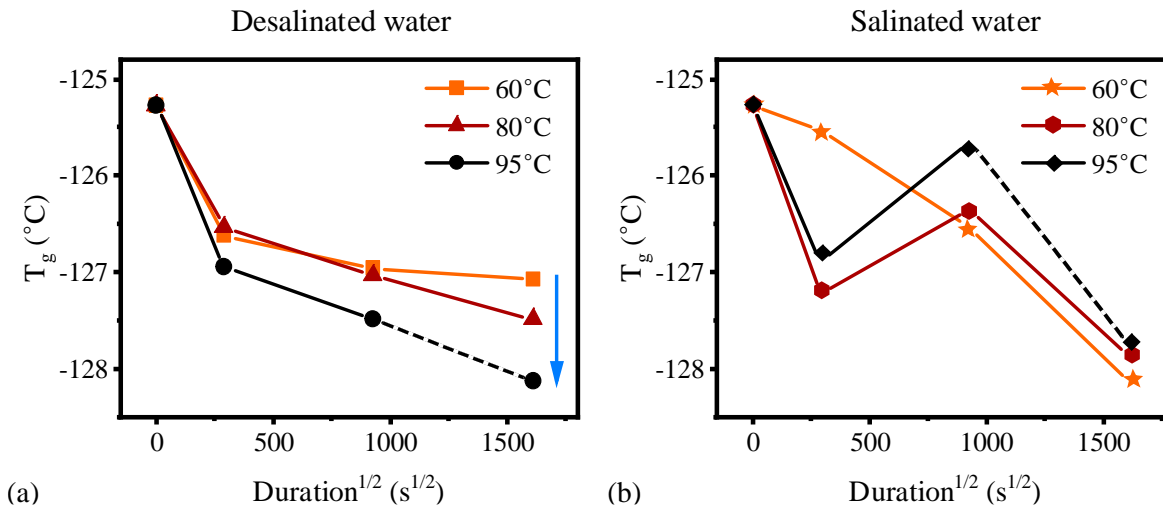


Figure 3.16 Glass transition temperature changed after (a) desalinated water, and (b) salinated water aging.

3.4 SEM analysis

SEM analysis has been done to study the morphology of tensile fracture surfaces of samples after aging in both desalinated and salinated environments. Figure 3.17 shows the failed samples with their respective SEM figures on fracture surfaces, which have been conducted on virgin and immersed specimens for 30 days at temperature 95°C in the medium of desalinated and salinated water. Scope of 10 μm and 2 μm was analyzed to study the detrimental effect induced by hydrolytic aging. As depicted, the virgin sample failed with an approximate 45° inclination, which is one of the characteristics of soft material's failure, shown in Figure 3.17(a). SEM figures also confirm this observation by presenting a high volume of microparticles on inclines failure lines on the failed sample surface, exhibited in Figure 3.17(b), (c). Furthermore, desalinated water caused the material to move even further in the direction of soft failure. As can be seen, in the most extensive case, the material almost lost its structure and became like gum, and then failed due to rupture. On the other hand, salinated water amazingly shifted the failure type to fracture type failure. One of the most important characteristics of this failure type is that

the failure surface is like a clean-cut perpendicular to the loading direction, which is almost the case in Figure 3.17(g). Furthermore, SEM pictures of the failed surface also add more certainty to this observation as they have relatively fewer particles on their surface in comparison to the virgin and desalinated case. This observation also can be concluded from the fact that elongation at break tends to increase in desalinated water while their trend is almost the opposite in the salinated environment. This trend is in agreement with SEM observations.

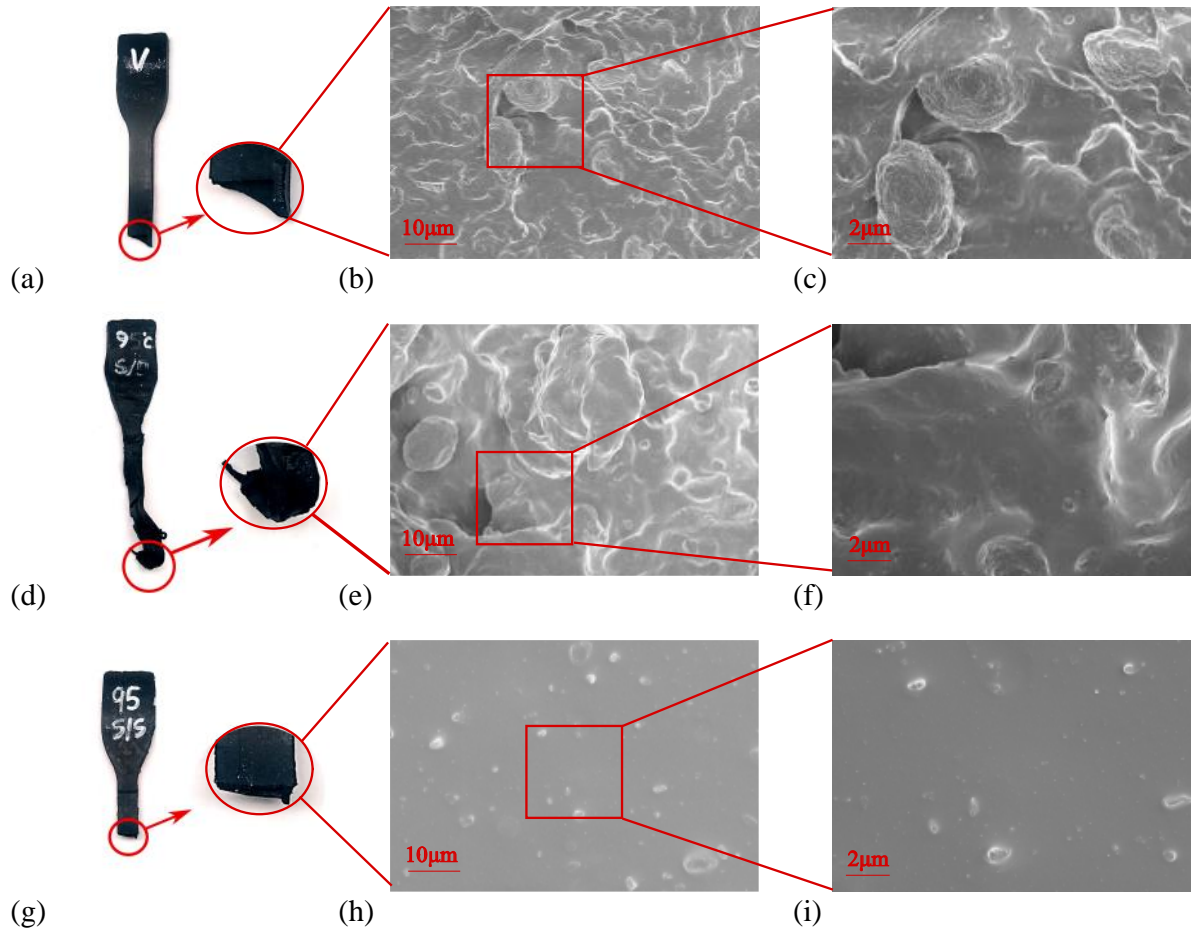


Figure 3.17 Failure samples and SEM micro-graphs of tensile fracture surfaces of (a), (b), and (c) virgin specimens, (d), (e), and (f) specimens aged within desalinated water at 95°C for 30 days, and (g), (h), and (i) specimens aged within salinated water at 95°C for 30 days.

4 Conclusion

This research investigated the effects of desalinated and saline water, which could cause varying degrees of damage to the macro-structural and mechanical properties of PDMS-based adhesives. The characterization and deterioration mechanisms have been studied and analyzed by water uptake, constitutive behaviors, FT-IR spectroscopy, DMA, and SEM tests.

Under desalinated water, water uptake increases with time and temperature. To some extent, a gradual increment of water uptake causes an increase in elongation at break and a reduction of the tensile strength of aged specimens. This increase in elongation at break is a result of the consistent expansion of the plasticization phenomenon, which has been verified by decreasing T_g and morphological graphs. Conversely, in the case of saline water, water uptake reduces after a certain time which could be considered the effects of protection barrier by precipitation of sea salt and leaching as a result of cross-link and chain scission. The generation of chemical cross-links gave rise to the brittle behaviors of constitutive behaviors, which has been approved with FT-IR spectroscopy and SEM results. It is noteworthy to mention that in the saline solution, degradation of materials is more overt in one-day aging which might be owing to a higher pH value and comparatively gentle in its reduction during further aging due to generation of the mentioned protection barrier.

This investigation is anticipated to gain a comprehensive knowledge of hydrolytic aging of PDMS-based adhesives to cope with harsh environments for further applications.

5 *Future Work*

In the field of modeling the constitutive behaviors of rubber-like materials, two essential parameters will be considered: damage induced by environments and cyclic deformation. In this study, the inelastic properties keep constancy if PDMS-based adhesives through 95°C could be regarded as annihilation. In other words, the damage induced by deformation is constant, which can be indicated that the environmental damages during cyclic loading have been decomposed. From this point of view, these two parameters can be interpreted as a correlation of independency. The future model will investigate whether this hypothesis is validated or not.

BIBLIOGRAPHY

Bibliography

- Accettola, F. a. (2008). Siloxane removal from biogas by biofiltration: biodegradation studies. *Clean Technologies and Environmental Policy*, 211--218.
- Aglan, H. a. (2008). Effect of UV and hygrothermal aging on the mechanical performance of polyurethane elastomers. *Journal of Applied Polymer Science*, 558--564.
- Alessi, S. a. (2014). Effect of hydrothermal ageing on the thermal and delamination fracture behaviour of CFRP composites. *Composites Part B: Engineering*, 67, 145--153.
- Antosik, A. K. (2018). Aging of silicone pressure-sensitive adhesives. *Polymer Bulletin*, 1141--1147.
- Awaja, F. a. (2016). Cracks, microcracks and fracture in polymer structures: Formation, detection, autonomic repair. *Progress in Materials Science*, 83, 536--573.
- Awaja, F. a. (2016). Cracks, microcracks and fracture in polymer structures: Formation, detection, autonomic repair. *Progress in Materials Science*, 536--573.
- Badertscher, M. a. (2009). *Structure Determination of Organic Compounds: Tables of Spectral Data*. Springer.
- Bahrololoumi, A. a. (2020). A multi-physics constitutive model to predict quasi-static behaviour: Hydrolytic aging in thin cross-linked polymers. *International Journal of Plasticity*, 102676.
- Barbosa, A. P. (2017). Accelerated aging effects on carbon fiber/epoxy composites. *Composites Part B: Engineering*, 110, 298--306.
- Barral, L. a.-B. (2000). Physical aging of a tetrafunctional/phenol novolac epoxy mixture cured with diamine. DSC and DMA measurements. *Journal of thermal analysis and calorimetr*, 391--399.
- Bele, A. a. (2016). Aging behavior of the silicone dielectric elastomers in a simulated marine environment. *RSC advances*, 6, 8941--8955.
- Borek, J. a. (1998). Influence of the plasticization on free volume in polyvinyl chloride. *Journal of Polymer Science Part B: Polymer Physics*, 1839--1845.
- C1246-17, A. (2012). *Standard Test Method for Effects of Heat Aging on Weight Loss, Cracking, and Chalking of Elastomeric Sealants After Cure*. West Conshohocken, PA: ASTM.

- Capiel, G. a. (2017). Water diffusion and hydrolysis effect on the structure and dynamics of epoxy-anhydride networks. *Polymer Degradation and Stability*, 143, 57--63.
- Celina, M. C. (2013). Review of polymer oxidation and its relationship with materials performance and lifetime prediction. *Polymer Degradation and Stability*, 98, 2419--2429.
- Chaudhry, A. a. (2001). Characterisation and oxidative degradation of a room-temperature vulcanised poly (dimethylsiloxane) rubber. *Polymer degradation and Stability*, 73, 505--510.
- Chen, Y. a. (2019). Super-hydrophobic, durable and cost-effective carbon black/rubber composites for high performance strain sensors. *Composites Part B: Engineering*, 176, 107358.
- Choi, S.-S. a.-H. (2010). Water swelling behaviors of silica-reinforced NBR composites in deionized water and salt solution. *Journal of Industrial and Engineering Chemistry*, 16, 238--242.
- D1141-98, A. (2008). *Standard Practice for the Preparation of Substitute Ocean Water*. West Conshohocken, PA: ASTM International.
- D412, A. (2006). *Standard test methods for vulcanized rubber and thermoplastic elastomers--tension*. West Conshohocken, PA: ASTM book of standards.
- Dangla, R. a. (2010). Microchannel deformations due to solvent-induced PDMS swelling. *Lab on a Chip*, 2972--2978.
- De Buyl, F. (2001). Silicone sealants and structural adhesives. *International Journal of Adhesion and Adhesives*, 21, 411--422.
- Deroine, M. a.-M.-Y. (2014). Accelerated ageing of polylactide in aqueous environments: comparative study between distilled water and seawater. *Polymer degradation and stability*, 108, 319--329.
- Diani, J. a. (2009). A review on the Mullins effect. *European Polymer Journal*, 45, 601--612.
- Diani, J. a. (2009). A review on the Mullins effect. *European Polymer Journal*, 45, 601--612.
- Dorfmann, A. a. (2004). A constitutive model for the Mullins effect with permanent set in particle-reinforced rubber. *International Journal of Solids and Structures*, 41, 1855--1878.
- Dorfmann, A. a. (2004). A constitutive model for the Mullins effect with permanent set in particle-reinforced rubber. *International Journal of Solids and Structures*, 41, 1855--1878.

- Dunson, D. (2017). Characterization of Polymers using Dynamic Mechanical Analysis (DMA).
- E.M.Dennenberg. (1966). Trans. Inst. Rubber Znd. 42(T26).
- Eesaee, M. a. (2014). Effect of nanoclays on the mechanical properties and durability of novolac phenolic resin/woven glass fiber composite at various chemical environments. *Composites Part A: Applied Science and Manufacturing*, 149--158.
- Fayolle, B. a. (2008). degradation-induced embrittlement in semi-crystalline polymers having their amorphous phase in rubbery state. *Journal of materials science*, 43, 6999--7012.
- G"opferich, A. (1996). Mechanisms of polymer degradation and erosion. *Biomaterials*, 17, 103--114.
- Gao, X. a. (2015). Inelastic behaviour of bacterial cellulose hydrogel: in aqua cyclic tests. *Polymer Testing*, 44, 82--92.
- Grassie, N. a. (1978). The thermal degradation of polysiloxanes—I. Poly (dimethylsiloxane). *European polymer journal*, 14, 875--884.
- Gugliuzza, A. a. (2007). PVDF and HYFLON AD membranes: Ideal interfaces for contactor applications. *Journal of Membrane Science*, 300, 51--62.
- Gulmine, J. a. (2003). Degradation profile of polyethylene after artificial accelerated weathering. *Polymer degradation and stability*, 79, 385--397.
- Hagen, R. a. (1996). Effects of the type of crosslink on viscoelastic properties of natural rubber. *Journal of Polymer Science Part B: Polymer Physics*, 1997--2006.
- Harwood, J. a. (1971). Stress-softening and reinforcement of rubber. *Journal of Macromolecular Science, Part B: Physics*, 5, 473--486.
- Huang, L. a. (2019). Pseudo-Elastic Analysis with Permanent Set in Carbon-Filled Rubber. *Advances in Polymer Technology*, 2019.
- Hutchinson, J. M. (1995). Physical aging of polymers. *Progress in polymer scienc*, 20, 703--760.
- Hutchinson, J. M. (1995). Physical aging of polymers. *Progress in polymer science*, 703--760.
- Izdebska, J. a. (2015). *Printing on polymers: fundamentals and applications*. William Andrew.
- Jagger, T. A. (2003). Analysis of the properties of silicone rubber maxillofacial prosthetic materials. *Journal of dentistry*, 31, 67-74.
- Keshavaraj, R. a. (1993). Modeling of crosslinking mechanism when structural silicone sealants are subjected to moisture. *Polymer-Plastics Technology and Engineering*, 579--593.

- Keshavaraj, R. a. (1994). Effects of moisture on structural silicone rubber sealants used in window glazing applications. *Construction and building materials*, 227-232.
- Khabbaz, F. a.-C. (1999). Chemical and morphological changes of environmentally degradable polyethylene films exposed to thermo-oxidation. *Polymer Degradation and Stability*, 63, 127--138.
- Le Gac, P.-Y. a. (2012). Ageing mechanism and mechanical degradation behaviour of polychloroprene rubber in a marine environment: Comparison of accelerated ageing and long term exposure. *Polymer Degradation and Stability*, 97, 288--296.
- Lee, J. a.-H. (2013). Effect of thermal treatment on the chemical resistance of polydimethylsiloxane for microfluidic devices. *Journal of Micromechanics and Microengineering*, 23, 035007.
- Levine, H. a. (1988). *Water Science Reviews 3: Water Dynamics*. Cambridge University Press.
- Lewicki, J. P. (2009). The thermal degradation behaviour of polydimethylsiloxane/montmorillonite nanocomposites. *Polymer Degradation and Stability*, 94, 1548--1557.
- Lewicki, J. P. (2009). The thermal degradation behaviour of polydimethylsiloxane/montmorillonite nanocomposites. *Polymer Degradation and Stability*, 94, 1548--1557.
- Li, J. a.-K. (2012). A reliability study of adhesion mechanism between liquid crystal polymer and silicone adhesive. *Microelectronics Reliability*, 2962--2969.
- Li, X. a. (2004). Sea-water effects on foam-cored composite sandwich lay-ups. *Composites Part B: Engineering*, 35, 451--459.
- Ma, G. a. (2018). Effects of water, alkali solution and temperature ageing on water absorption, morphology and mechanical properties of natural FRP composites: Plant-based jute vs. mineral-based basalt. *Composites Part B: Engineering*, 153, 398--412.
- Malla, R. B. (2011). Temperature aging, compression recovery, creep, and weathering of a foam silicone sealant for bridge expansion joints. *Journal of materials in civil engineering*, 287--297.
- Mathew, A. P. (2001). Studies on the thermal stability of natural rubber/polystyrene interpenetrating polymer networks: thermogravimetric analysis. *Polymer Degradation and Stability*, 72, 423--439.
- McCaig, M. a. (1999). Effect of UV crosslinking and physical aging on the gas permeability of thin glassy polyarylate films. *Polymer*, 7209--7225.

- Mohammadi, H. a. (2019). A micro-mechanical approach to model thermal induced aging in elastomers. *International Journal of Plasticity*, 118, 1--16.
- Montemayor, C. (2014). Exploring high-temperature reliability limits for silicone adhesives. *SMT Magazine*, 34--46.
- Montes, J. C.-M. (2012). Ageing of polyethylene at raised temperature in contact with chlorinated sanitary hot water. Part I--Chemical aspects. *Polymer degradation and stability*, 97, 149--157.
- Odegard, G. a. (2011). Physical aging of epoxy polymers and their composites. *Journal of polymer science Part B: Polymer physics*, 49, 1695--1716.
- Rahman, M. a. (2004). The plasticizer market: an assessment of traditional plasticizers and research trends to meet new challenges. *Progress in polymer science*, 29, 1223--1248.
- Sang, L. a. (2018). Effects of hydrothermal aging on moisture absorption and property prediction of short carbon fiber reinforced polyamide 6 composites. *Composites Part B: Engineering*, 153, 306--314.
- Sawpan, M. A. (2012). Glass transitions of hygrothermal aged pultruded glass fibre reinforced polymer rebar by dynamic mechanical thermal analysis. *Materials & Design*, 272--278.
- Sedenkova, I. a. (2008). Thermal degradation of polyaniline films prepared in solutions of strong and weak acids and in water--FTIR and Raman spectroscopic studies. *Polymer Degradation and Stability*, 93, 2147--2157.
- Su, X. a. (2018). Tough, resilient and pH-sensitive interpenetrating polyacrylamide/alginate/montmorillonite nanocomposite hydrogels. *Carbohydrate polymers*, 197, 497--507.
- Sun, Y. K. (2018). Study of Tensile Bond Strength for Structural Silicone Sealants after Artificial Accelerated Aging. *Key Engineering Materials*, 13--18.
- Sundararajan, P. (2002). Crystalline morphology of poly (dimethylsiloxane). *Polymer*, 43, 1691--1693.
- Tavares, A. C. (2003). The effect of accelerated aging on the surface mechanical properties of polyethylene. *Polymer Degradation and Stability*, 81, 367--373.
- Verma, A. R. (2017). Accelerated aging studies of silicon-rubber based polymeric insulators used for HV transmission lines. *Polymer Testing*, 62, 124--131.
- Wang, M. a. (2016). The hygrothermal aging process and mechanism of the novolac epoxy resin. *Composites Part B*, 107, 1--8.

Warrick, E. a. (1979). Silicone elastomer developments 1967--1977. *Rubber chemistry and technology*, 52, 437--525.

Xiang, K. a. (2012). Accelerated thermal ageing studies of polydimethylsiloxane (PDMS) rubber. *Journal of Polymer Research*, 19, 9869.

Yanagibashi, N. a. (1990). Adhesive device for application to body tissue. *Google Patents*.